Int J Clin Exp Pathol 2015;8(7):8311-8335
www.ijcep.com /ISSN:1936-2625/IJCEP0010165

Original Article

Papillary renal cell carcinoma: a clinicopathological and whole-genome exon sequencing study

Kunpeng Liu[1*], Yuan Ren[1*], Lijuan Pang[1], Yan Qi[1], Wei Jia[1], Lin Tao[1], Zhengyan Hu[1], Jin Zhao[1], Haijun Zhang[2], Li Li[2], Haifeng Yue[3], Juan Han[3], Weihua Liang[4], Jianming Hu[1], Hong Zou[1*], Xianglin Yuan[3], Feng Li[1*]

[1]Department of Pathology, School of Medicine, Shihezi University, Key Laboratory of Xinjiang Endemic and Ethnic Diseases, Ministry of Education of China; [2]Department of Pathology, First Affiliated Hospital of Medical School, Shihezi University, China; [3]Community hospital of Shihezi University, Shihezi City, Xin Jiang, China; [4]Tongji Hospital Cancer Center, Tongji Medical College, Huazhong University of Science and Technology, China. [*]Equal contributors.

Received May 12, 2015; Accepted June 26, 2015; Epub July 1, 2015; Published July 15, 2015

Abstract: Papillary renal cell carcinoma (PRCC) represents the second most common histological subtype of RCC, and comprises 2 subtypes. Prognosis for type 1 PRCC is relatively good, whereas type 2 PRCC is associated with poor clinical outcomes. The aim of the present study was to evaluate the clinicopathological and mutations characteristics of PRCC. Hence, we reported on 13 cases of PRCC analyzed using whole-exome sequencing. Histologically, type 2 PRCC showed a higher nuclear grade and lymphovascular invasion rate versus type 1 PRCC ($P < 0.05$). Immunostaining revealed type 1 PRCC had higher CK7 and lower Top IIα expression rates ($P < 0.05$). Whole-exome sequencing data analysis revealed that the mutational statuses of 373 genes (287 missense, 69 silent, 6 nonsense, and 11 synonymous mutations) differed significantly between PRCC and normal renal tissues ($P < 0.05$). Functional enrichment analysis was used to classify the 287 missense-mutated genes into 11 biological process clusters (comprised of 61 biological processes) and 5 pathways, involved in cell adhesion, microtubule-based movement, the cell cycle, polysaccharide biosynthesis, muscle cell development and differentiation, cell death, and negative regulation. Associated pathways included the ATP-binding cassette transporter, extracellular matrix-receptor interaction, lysosome, complement and coagulation cascades, and glyoxylate and dicarboxylate metabolism pathways. The missense mutation status of 19 genes differed significantly between the groups ($P < 0.05$), and alterations in the EEF1D, RFNG, GPR142, and RAB37 genes were located in different chromosomal regions in type 1 and 2 PRCC. These mutations may contribute to future studies on pathogenic mechanisms and targeted therapy of PRCC.

Keywords: Papillary renal cell carcinoma, whole-exome sequencing, gene mutation

Introduction

Renal cell carcinoma (RCC) accounts for approximately 90% of all renal malignancies. Papillary RCC (PRCC), the second most common RCC subtype, accounting for approximately 10% of all cases, is a renal parenchyma malignant tumor with papillary or tubulopapillary architecture that presents as type 1 or 2 PRCC; type 1 PRCC is composed of single layered small cell and scanty cytoplasm, type 2 PRCC is characterized by pseudostratified large cells and eosinophilic cytoplasm is a renal parenchyma malignant tumor with papillary or tubulopapillary architecture [1]. Based on the cytologic and histologic features, PRCC can be divided into two subtypes, types 1 and 2 [2]. Type 1 PRCC is generally considered to have a better prognosis than type 2 PRCC, although no consensus regarding the standard treatment for metastatic PRCC exists [3-7].

Molecular genetic studies are highly important in diagnosis and prognosis evaluation, and may provide treatment directions. MET locates at 7q, and its mutation relates to susceptibility to PRCC [8]. Mutations of MET have been identified to cause hereditary PRCC, and occur in a small proportion of sporadic PRCC and a greater number show somatic copy number gains involving chromosome 7q [8, 9]. In addition, leucine-rich repeat kinase 2 (LRRK2) is overex-

pressed and amplified in PRCC. MET and LRRK2 have a synergistic effect during tumor growth via the mTOR and STAT3 pathway [10]. The exome BeadChip can not only identify gene mutations, but also identify diagnostic and therapeutic oncogenes and tumor suppressor genes. Although the pathologic and immunophenotypic of PRCC have been investigated, whole-genome exon sequencing reports are limited. Therefore, we here examined the clinicopathological and gene mutation characteristics of PRCC by a combination of immunohistochemistry and exon chip analyses.

Materials and methods

Specimens

The study contained 13 paraffin-embedded PRCCs and 18 normal kidney tissues. 13 tumors consisted of 6 case of type 1 and 7 case of type 2 PRCC. All tissues were obtained from the archives of the Department of Pathology, School of Medicine, Shihezi University. After asked for the view of the patients and the Institutional Research Ethics Committee, we make a collection of the clinicopathological data for these cases in the patients' medical records. All specimens were observed by two independent pathologists. Nuclear grading was done according to the Fuhrman nuclear grade system. Tumor stages were according to the 2010 TNM (T = Tumor, N = Node, M = Metastases) classification of the American Joint Committee on Cancer.

Immunohistochemistry (IHC)

IHC staining was performed on 4 μm thick formalin-fixed, paraffin-embedded tissue sections by the 2-step Envision technique (Dako, Denmark). The primary antibodies included cluster of differentiation (CD) 10 (GT200410, 1:100), cytokeratin (CK) (AE1/AE3, 1:100), vimentin (Vim3B4, 1:100), CD117 (1:300), alpha-methylacyl-CoA racemase (AMACR), Top IIα, MDM2, p53, (13H4, 1:100), and CK7 (OV-TL12/30, 1:50), and purchased from Dako company. Negative or positive control was set up on the basis of antibodies.

DNA extraction

Total DNA was isolated from the 13 cases of PRCC and 18 cases of normal kidney tissue samples by using a standard phenol/chloroform extraction method. The quantity of DNA was measured by reading A260/280 ratios by spectrophotometer. When A260/280 ratios located range 1.8 to 2.0, DNA was available. Extractions were stored at -80°C until they were labeled by nick translation.

Whole-exome sequencing

A total of 1 μg of DNA from each of the 13 PRCC tissues and 18 normal kidney tissues were labeled with Illumina reagents and hybridized to Human Exome BeadChips (Illumina, USA). The quality assessment was performed by Illumina Expression Console software. Compared with normal renal tissues, the mutative genes were identified the mutated genes by significance analysis of microarrays (SAM) algorithm in PRCC tissues. The mutative genes associated with cell cycle regulation and other biological functions were determined by Gene Ontology biological process (Gene Ontology BP) enrichment of the classification analysis. The pathways associated with PRCC were confirmed by the Kyoto Encyclopedia of Genes and Genomes database (KEGG).

Statistical analysis

All statistical calculations were done using SPSS 17.0. Difference of measurement data was compared with single factor analysis of variance. Count data were analyzed using Fisher's exact test. Classification enrichment of gene function and pathway were used to analyze gene function (Gene Ontology of Biological Processes, Molecular function) by DAVID database and KEGG Database. P value < 0.05 was a difference in statistics.

Results

Clinical features

The clinical characteristics of type 1 and type 2 PRCC are summarized in **Table 1**. In this cohort, 7 patients were men and 6 were women (1.2 male/female ratio); mean age was 53.9 (range from 26 to 74); the average age of the patients was 61.5 (range from 48 to 74) with type 1 PRCC, 47.4 (range from 26 to 63) with type 2 PRCC. The male-to-female ratio, the mean age of the patients, and metastasis were not significantly different between the two groups. In the

Table 1. Distribution of analyzed clinicopathologic features and outcome of type 1 and type 2 PRCC

Characteristics		Type 1	Type 2	*P* value
No. of patients		6	7	
Age of patients	Mean ± SD	61.5 ± 11.8	47.4 ± 13.7	0.075
	Range	48-74	26-63	
Sex of patients	Male	3	4	
	Female	3	3	0.617
Metastasis	Positive	0	1	0.538
Tumor size (cm)	Mean ± SD	6.92 ± 3.06	7.27 ± 3.10	0.840
	Range	3.5-11	3.9-13	
Fuhrman grade	Low (1-2)	6	2	
	High (3)	0	5	0.049
Lymphovascular invasion	Negative	6	3	
	Positive	0	4	0.049
stage	I-II	6	4	
	III -IV	0	3	0.122
Outcome	Dead	5 (5/6)		

P value: type 1 PRCC vs. type 2 PRCC; Fisher's exact test.

13 cases, 3 were asymptomatic, 6 were presented with osphyalgia, and 4 were presented with hematuria. Ultrasonic examination and Computed tomography (CT) showed inhomogeneous mass, as the tumor mass often had hemorrhage, necrosis, or cystic degeneration. Follow-up found the tumor related survival rate was 82.7% (5/6) for the patients with type 1 and 28.6% (2/7) for those with type 2 PRCC. According to 2010 AJCC staging criteria, 6 neoplasms presented at stage 1, 4 at stage 2, 3 at stage 3, 0 at stage 4.

Histopathology

The differences of histopathology between the two types were described in **Table 1**. All tumors were located in unilateral renal parenchyma; Mean tumor size, calculated on the maximum diameter, was 7.11 cm (range from 3.5 to 13 cm); it was no difference between the two types. Tumor color are gray, gray yellow, gray red, or colorful; necrosis and hemorrhage could be observed in 4 cases grossly. Microscopically, the tumor was mainly composed of the different proportion of papillary and tubular structure. They were composed of cells arranged on a delicate fibrovascular core. The cytoplasm may be basophilic, eosinophilic, or sometimes partially clear. 6 (6/13) cases were diagnosed as type 1 (**Figure 1A**) and 7 (7/13) cases were type 2 PRCC (**Figure 1B**) by their appearance under a microscope. Type 2 PRCC had higher nuclear grade (P = 0.049) and Lymphovascular invasion in relative to type 1 (P = 0.049).

Immunohistochemistry

Results of immunohistochemical staining were summarized in **Table 2**. All PRCC expressed AMACR (**Figure 1C**), CK7 positive expression rate of type 1 PRCC (6/6) was higher in compared with type 2 (2/7) (P = 0.016). In contrast, Top IIα immunoreactivity was negative (0/6) in type 1 PRCC, while the majority of type 2 PRCC (4/7) were positive for Top IIα (P = 0.049).

Whole-exome sequencing

In the whole-exome sequencing data analysis, the mutational status of 373 genes was found to be significantly different (P < 0.05) between PRCC and normal renal tissues. In PRCC tissues, 287 missense, 69 silent, 6 nonsense, and 11 synonymous mutations were detected (**Table 3**). In the functional enrichment analysis, the 287 missense-mutated genes were classified into 11 biological process clusters (comprised of 61 biological progresses) and 5 pathways (P < 0.05) (**Table 4**; **Figure 2A**). Mutated genes in PRCC tissues were mainly involved in cell adhesion, microtubule-based movement, cell cycle process, polysaccharide biosynthetic process, tissue morphogenesis, muscle cell development, cell death, differentiation maintenance of organ identity, negative regulation, fertilization, synapsis. Associated pathways included ABC transporters (ATP-binding cassette transporter), ECM (extracellular matrix)-receptor interaction, Lysosome, Complement and coagulation cascades, and Glyoxylate and dicarboxylate metabolism.

The missense mutation status of 19 genes was significantly different (P < 0.05) between the type 1 PRCC C and type 2 PRCC groups (**Table 5**). Alterations in EEF1D, RFNG, GPR142, and RAB37 genes were located in different chromosomal regions in the type 1 PRCC C and type 2 PRCC groups.

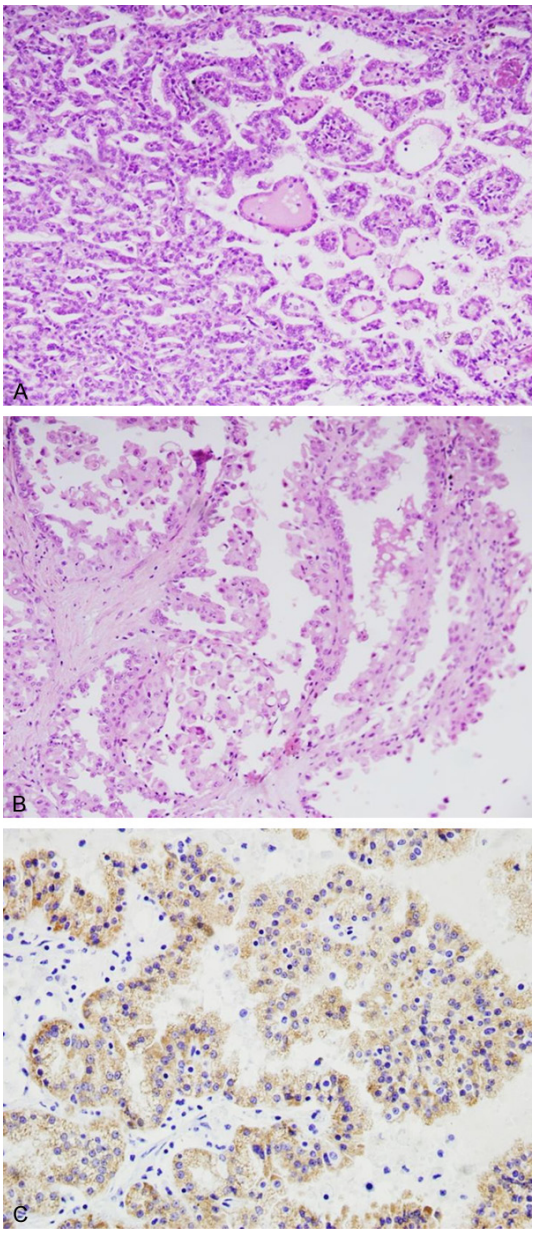

Figure 1. Microscopic and immunohistochemical findings in PRCC. A. Type 1 PRCC was papillae covered by small tumor cells with scanty and basophilic cytoplasm and round nucleus, arranged in a single layer on papillary basement membrane. (H&E, × 200); B. Type 2 PRCC was pseudostratified ciliated columnar epithelium on papillary cores, often with abundant and eosinophilic cytoplasm, large nuclei and prominent nucleoli (H&E, × 200); C. Immunohistochemically, PRCC showed diffuse intense plasma membrane staining for AMACR. (× 200).

Discussion

PRCC is the second most prevalent renal tumor after renal clear cell carcinoma [1]. PRCC can be divided into two types based on the histomorphological features. The onset age and sex of PRCC patients are similar to ccRCC patients, with a peak incidence in 50-70-year-old men [1, 11]. Herein, the average age of the patients was 53.9 years (range, 26-74 years). Compared with type 1, the mean age of type 2 PRCC patients was approximately 14 years lower (57.4 vs. 61.5 years), which is consistent with the results of previous studies [12, 13].

Pathologically, type 2 tumors showed a higher Fuhrman grade (P = 0.049) and lymphovascular invasion (P = 0.049) than type 1, which have both been identified as prognostic factors [14, 15], suggesting poorer outcomes in type 2 PRCC patients. While some studies have reported no clear correlation between PRCC type and prognosis [16, 17], most have shown that type 1 PRCC has a better prognosis compared to type 2 [11-13, 18]. Moreover, compared with the overall survival rates of patients with type 1 PRCC, those of type 2 PRCC were lower in this study, suggesting that tumor classification is indeed helpful for evaluating the prognosis of PRCC patients.

Immunohistochemically, all 13 tumors showed strong positivity for AMACR, while CK7 and Top IIα were overexpressed in types 1 and 2 PRCC, respectively. This is consistent with previous reports [1, 19-21], suggesting that AMACR, CK7, and Top IIα are useful for the classification, diagnosis, and differential diagnosis of PRCC. Importantly, increased Top IIα expression correlates to poorer prognosis of various tumors, such as breast and colon cancer [22, 23], and some researchers found that Top IIα expression is increased in type 2 PRCC with higher Fuhrman nuclear grade, and that the level of Top IIα positively correlates with tumor invasion [24]. Herein, type 1 PRCC did not express Top IIα, whereas 57.1% of type 2 PRCC cases did (4/7), indicating that Top IIα not only contributes to the differential diagnosis, classification, and prognosis of PRCC, but may also play a role in its development.

In order to further detect gene mutations, we analyzed the exon of 13 PRCC and 18 normal kidney tissues by whole-genome exon sequencing. In the cluster analysis, we identified 10 enriched clusters (**Table 4**), with the frequency of gene mutations related to the cell division cycle being the highest (**Figure 2A**). Cell division is an important process, and problems during

Table 2. Immunohistochemical analyses of CK, CD10, Vimentin, AMACR, CK7, CD117, Top IIα, MDM2, and p53 in PRCC

Antigen	PRCC	Type 1	Type 2	*P* value
	% (n)	% (n)	% (n)	% (n)
CK	84.6 (11/13)	83.3 (5/6)	85.7 (6/7)	
CD10	30.8 (4/13)	50 (3/6)	14.3 (1/7)	
Vimentin	30.8 (4/13)	33.3 (2/6)	28.6 (2/7)	
AMACR	100 (13/13)	100 (6/6)	100 (7/7)	
CK7	61.5 (8/13)	100 (6/6)	28.6 (2/7)	0.016
CD117	30.8 (4/13)	33.3 (2/6)	28.6 (2/7)	
Top IIα	30.8 (4/13)	0 (0/6)	57.1 (4/7)	0.049
MDM2	0 (0/13)	0 (0/6)	0 (0/7)	
P53	30.8 (4/13)	7.7 (1/6)	42.9 (3/7)	

P value: type 1 PRCC vs. type 2 PRCC; Fisher's exact test.

the processing can result in abnormal cell division, proliferation, differentiation, and senescence. Numerous growth factors, cytokines, hormones, and cancer gene products regulate metabolism by influencing the cell division cycle. Meanwhile, the expression of many genes is restricted by the cell division cycle. Thus, our results suggest that these genes may play important roles in the occurrence and development of PRCC.

In the cell division cycle cluster, many interesting genes, such as MAP3K11 and KIF11, were identified. The protein encoded by MAP3K11 may activate MAPK8/JNK kinase, which regulates the JNK signal pathway and activates NF-kappa B signaling pathway, mediated by GTPases and CDC42, which in turn regulates cell proliferation and apoptosis [25, 26]. Recently, MAP3K11 has been shown to play a role in the development of prostate, breast, and gastric cancers through interfering with cell proliferation and apoptosis [27-29]. KIF11 encodes a kinesin spindle protein, a member of the kinesin superfamily of microtubule-based motors, and plays a critical role in mitosis through mediation of centrosome separation and bipolar spindle assembly and maintenance. Reduced KIF11 expression leads to cell cycle arrest at mitosis and formation of monoastral microtubule arrays, and, ultimately, to tumor cell death [30-32]. Sun et al. [33] reported that KIF11 overexpression correlated with nuclear grade ($P = 0.019$), stage ($P = 0.007$), and tumor size ($P = 0.033$) in RCC, and as type 2 PRCC shows higher nuclear grade and stage and worse prognosis than type 1, it can be speculated that it is associated with MAP3K11 and KIF11 mutations; however, further studies are needed to confirm this hypothesis.

The pathway enrichment analysis revealed 5 related pathways (**Table 4**), with the "ABC transporter" pathway being the most significant pathway in PRCC. The ABC transporters form one of the largest known protein families, and couple ATP hydrolysis to active transport of a wide variety of substrates such as lipids, sterols, proteins, and drugs. Numerous studies have shown that this pathway plays an important role in the development of multidrug resistant tumors [34-36]. These proteins can actively transport drugs from the intracellular to extracellular compartments, thereby reducing the intracellular concentration of drugs. Zhao et al. [36] showed that ABCC4 was highly expressed in lung cancer, and that reduced ABCC4 expression could inhibit tumor growth and proliferation. Walsh et al. [37] showed that ABCB1 and ABCC1 up regulation resulted in the development of multi-drug resistant RCC, and Hour et al. [38] reported that ABCD1 down regulation may be involved in renal tumorigenesis. Therefore, we inferred that mutations in the ABC pathways may reduce the effectiveness of chemotherapy drugs and promote the growth and proliferation of PRCC cells, and that inhibition of the ABC transporters may increase the efficacy of chemotherapy and slow down the development of PRCC.

Additionally, in the 5 related pathways, "ECM-receptor interaction" mutations commonly occurred (**Figure 2B**), with the mutation frequency of the collagen family genes being the highest. COL4A1 encodes the major type IV alpha collagen chain of basement membranes, which plays an essential role in tumorigenesis, growth, and metastasis. Delektorskaya et al. [39] suggested that type IV collagen shows different degrees of loss in colorectal cancer, which significantly correlated with the risk of metastasis. Others have found that type IV collagen promotes tumor cell migration and invasion in pancreatic cancer, and that the level of serum type IV collagen in these patients positively correlated with the risk of recurrence [40, 41]. Moreover, RCC cells can also produce type IV collagen as a means to promote tumor inva-

Table 3. The 287 genes containing missense mutations detected in the PRCC tissues ($p < 0.05$)**

Chr	SNP_name	Alleles	Gene	p	Mutation(s)
1	exm112317	[T/C]	CD1C	0.039215686	Missense_A118V
1	exm103938	[T/C]	UBAP2L	0.027634131	Missense_A642V, Missense_A642V
1	exm134287	[A/C]	ASPM	0.049773756	Missense_A663S, Missense_A663S
1	exm112233	[C/G]	CD1A	0.033333333	Missense_C68W
1	exm135632	[A/G]	CAMSAP2	0.032967033	Missense_D257N
1	exm124480	[T/C]	CENPL	0.045454545	Missense_D285G, Missense_D285G, Missense_D331G
1	exm131535	[A/G]	HMCN1, MIR548F1	0.016983017	Missense_E2893G, Silent
1	exm113728	[C/G]	MNDA	0.018181818	Missense_E41Q
1	exm131223	[A/G]	HMCN1	0.022977023	Missense_E494K
1	exm127218	[C/G]	AXDND1	0.014705882	Missense_E991Q
1	exm140251	[A/G]	ZC3H11A	0.032967033	Missense_G233S
1	exm100981	[T/C]	CRNN	0.047385621	Missense_G480S
1	exm131714	[T/C]	HMCN1, MIR548F1	0.047619048	Missense_H4084Y, Silent
1	exm121615	[T/C]	C1orf114	0.047619048	Missense_I37V
1	exm112921	[A/G]	OR10X1	0.030969031	Missense_I60T
1	exm100957	[T/A]	FLG2	0.009960474	Missense_L168F
1	exm139949	[T/C]	OPTC	0.013931889	Missense_L268P
1	exm142351	[A/G]	LEMD1	0.044117647	Missense_P25S, Missense_P25S, Missense_P25S, Silent, Missense_P25S
1	exm113801	[T/C]	MNDA	0.028571429	Missense_P403L
1	exm138568	[A/C]	LGR6	0.045454545	Missense_P920T, Missense_P868T, Missense_P781T
1	exm118835	[T/C]	C1orf111	0.047619048	Missense_R217H
1	exm131074	[T/C]	SWT1	0.030701754	Missense_R656C, Missense_R656C
1	exm101773	[T/C]	SPRR4	0.033333333	Missense_R8W
1	exm1164	[T/C]	AGRN	0.008333333	Missense_T1044M
1	exm127753	[T/C]	CEP350	0.044117647	Missense_T1131I
1	exm131226	[T/C]	HMCN1	0.047619048	Missense_T512I
1	exm111790	[A/C]	FCRL3	0.027472527	Missense_V93G
1	exm118460	[C/G]	FCRLB	0.045454545	Missense_X427S
1	exm117119	[A/C]	KLHDC9	0.03250774	Silent, Silent, Missense_S171R, Missense_S171R
12	exm1053356	[A/G]	GALNT9	0.047619048	Missense_A152V, Missense_A518V
12	exm1025298	[A/C]	CEP290	0.029411765	Missense_D2396Y
12	exm1006156	[T/C]	KRT2	0.027472527	Missense_E376K
12	exm1054454	[T/C]	GOLGA3	0.028571429	Missense_G644D, Missense_G644D
12	exm1023832	[G/C]	OTOGL	0.010989011	Missense_H1239D
12	exm1002135	[T/G]	CERS5	0.030701754	Missense_I122L
12	exm1040411	[T/A]	RBM19	0.013986014	Missense_K351N, Missense_K351N, Missense_K351N
12	exm1038106	[T/C]	NAA25	0.024242424	Missense_K876R
12	exm1049484	[A/G]	NCOR2	0.047619048	Missense_P2215L, Missense_P2215L, Missense_P2225L
12	exm1049813	[A/G]	NCOR2	0.032967033	Missense_P535L, Missense_P535L, Missense_P536L

12	exm1024575	[C/G]	TMTC2	0.026315789	Missense_R139G
12	exm1006431	[T/C]	KRT77	0.045454545	Missense_R183Q
12	exm1034626	[A/G]	USP30	0.026315789	Missense_R206H
12	exm1042014	[A/G]	SRRM4	0.010989011	Missense_R223H
12	exm1036192	[A/G]	TCHP	0.047619048	Missense_R444H, Missense_R444H
12	exm1037483	[A/G]	SH2B3	0.034965035	Missense_R566Q
12	exm1029879	[A/G]	UTP20	0.015151515	Missense_R869K
12	exm1003394	[T/C]	GALNT6	0.008333333	Missense_S32N
12	exm1054936	[A/T]	ZNF268	0.022222222	Missense_S383T, Silent, Silent, Silent, Silent, Silent, Silent, Missense_S383T, Missense_S300T
12	exm1016108	[A/C]	INHBC	0.010989011	Missense_T166P
12	exm1053798	[T/C]	POLE	0.04743083	Missense_V1512I
12	exm1020377	[T/C]	MDM1	0.047619048	Missense_V348I, Missense_V383I
12	exm1050732	[A/G]	TMEM132C	0.004761905	Missense_V444I
12	exm1006093	[T/C]	KRT73	0.036521739	Missense_V61M
12	exm1013940	[T/C]	BAZ2A	0.045454545	Missense_V950I
12	exm1000913	[A/G]	FAM186B	0.028571429	Silent, Missense_P822S
12	exm1004123	[A/G]	KRT80	0.038461538	Silent, Missense_S445L
12	exm1042629	[T/C]	RAB35	0.012254902	Silent, Missense_V155I
12	exm1026178	[T/C]	CLLU1OS, CLLU1	0.047619048	Silent, Silent, Silent, Missense_T106M
13	exm1055958	[T/C]	N6AMT2	0.030701754	Missense_A140T
13	exm1060952	[A/G]	USPL1	0.045454545	Missense_E1010K
13	exm1074843	[A/C]	ABCC4	0.022222222	Missense_G187W, Missense_G187W
13	exm1062037	[A/C]	BRCA2	0.043956044	Missense_H2074N
13	exm1065617	[T/C]	NAA16	0.038461538	Missense_I547T
13	exm1057999	[T/C]	PARP4	0.027777778	Missense_I81V
13	exm1068871	[A/T]	SETDB2	0.01010101	Missense_K408I, Missense_K396I
13	exm1065317	[T/C]	ELF1	0.029411765	Missense_N58S, Missense_N58S
13	exm1065781	[A/G]	KIAA0564	0.035714286	Missense_P1173L
13	exm1070562	[A/C]	CKAP2	0.024242424	Missense_P127T, Missense_P128T
13	exm1061900	[G/C]	BRCA2	0.004761905	Missense_P655R
13	exm1064366	[A/G]	FREM2	0.022977023	Missense_R1668H
13	exm1069663	[T/C]	WDFY2	0.004995005	Missense_R168W
13	exm1062043	[A/G]	BRCA2	0.027634131	Missense_R2108H
13	exm1075739	[A/G]	FARP1	0.027472527	Missense_R411Q
13	exm1078359	[A/C]	SLC10A2	0.027777778	Missense_S171A
13	exm1081805	[A/G]	GRTP1	0.038461538	Missense_T227M
13	exm1079428	[C/G]	COL4A1	0.044117647	Missense_V7L
13	exm1082605	[A/G]	GAS6	0.015151515	Silent, Missense_S204L
14	exm1101474	[A/G]	FRMD6	0.032967033	Missense_A207T, Missense_A207T
14	exm1102020	[C/G]	TXNDC16	0.047619048	Missense_A398G, Missense_A403G
14	exm1107555	[A/G]	SYNE2	0.012383901	Missense_A6671T, Missense_A6648T, Missense_A305T, Missense_A179T
14	exm1129474	[A/G]	CDC42BPB	0.035714286	Missense_A983V

14	exm1098207	[C/G]	MIA2	0.043956044	Missense_D547H
14	exm1096768	[A/C]	FAM177A1	0.027777778	Missense_E64D, Missense_E87D
14	exm1115955	[T/A]	MLH3	0.021978022	Missense_F390I, Missense_F390I
14	exm1083818	[T/A]	OR4K13	0.049773756	Missense_I270N
14	exm1099035	[C/G]	FANCM	0.038461538	Missense_L526V
14	exm1098233	[T/C]	CTAGE5	0.036363636	Missense_P28S, Missense_P11S, Missense_P11S, Silent, Missense_P40S, Missense_P40S, Missense_P40S
14	exm1092597	[G/C]	REC8	0.022268908	Missense_P294R, Missense_P294R
14	exm1115047	[A/G]	LTBP2	0.045454545	Missense_P317L
14	exm1107750	[T/C]	MTHFD1	0.025641026	Missense_P328L
14	exm1125535	[T/C]	BDKRB2	0.027777778	Missense_R14C
14	exm1094536	[T/C]	CMA1	0.028571429	Missense_R151K
14	exm1084549	[T/C]	TEP1	0.045454545	Missense_R1772Q
14	exm1102594	[T/C]	CGRRF1	0.040959041	Missense_R185W
14	exm1090676	[T/C]	MYH6	0.038461538	Missense_R204H
14	exm1098547	[T/C]	FSCB	0.030969031	Missense_R385Q
14	exm1117477	[T/C]	POMT2	0.036363636	Missense_R421Q
14	exm1099301	[T/C]	MIS18BP1	0.038461538	Missense_R510Q
14	exm1129681	[T/C]	EXOC3L4	0.043956044	Missense_R560C
14	exm1122333	[T/C]	RIN3	0.032967033	Missense_R79W
14	exm1091339	[A/G]	DHRS2	0.035714286	Missense_R7Q, Missense_R7Q
14	exm1123266	[G/C]	UNC79	0.029411765	Missense_S1194C
14	exm1122077	[C/G]	ATXN3	0.012820513	##
14	exm1098992	[T/C]	FANCM	0.047619048	Missense_S175F
14	exm1120581	[T/G]	C14orf102	0.045454545	Missense_S35Y
14	exm1129309	[T/C]	AMN	0.047619048	Missense_S92L
14	exm1109913	[A/G]	ZFYVE26	0.008791209	Missense_T2352I
14	exm1121606	[A/G]	CATSPERB	0.045454545	Missense_T250M
14	exm1122447	[T/C]	RIN3	0.045454545	Missense_T638M
14	exm1104386	[A/G]	ARID4A	0.029411765	Missense_T779A, Missense_T779A, Missense_T779A
14	exm1100138	[T/C]	C14orf183	0.042105263	Missense_V263I
14	exm1134928	[A/G]	MTA1	0.022222222	Missense_V372I, Missense_V372I
14	exm1086223	[A/G]	ZNF219, C14orf176	0.028571429	Silent, Missense_E208K
15	exm1171367	[C/G]	TIPIN	0.034502262	Missense_A111G
15	exm1183486	[G/C]	FSD2	0.034965035	Missense_A129P
15	exm1156585	[A/G]	PPIP5K1	0.021708683	Missense_A1372V, Missense_A1374V, Missense_A1374V, Missense_A1399V
15	exm1169486	[T/C]	ANKDD1A	0.045454545	Missense_A141V
15	exm1154945	[G/C]	TTBK2	0.021978022	Missense_A519P
15	exm1147190	[T/C]	ATPBD4	0.044117647	Missense_D46N, Missense_D46N
15	exm1148492	[T/C]	PLCB2	0.011904762	Missense_E1110K
15	exm1152491	[T/C]	SPTBN5	0.035714286	Missense_E2614K
15	exm1148014	[A/G]	EIF2AK4	0.017857143	Missense_E556G

15	exm1194142	[A/G]	LRRK1	0.018181818	Missense_G1938D
15	exm1155304	[T/G]	TMEM62	0.017857143	Missense_G496V
15	exm1152787	[T/C]	SPTBN5	0.038461538	Missense_G800E
15	exm1179035	[C/G]	C15orf27	0.018181818	Missense_I141M
15	exm1152778	[T/C]	SPTBN5	0.027777778	Missense_K879E
15	exm1178328	[G/C]	IMP3	0.008791209	Missense_L182V
15	exm1171637	[G/C]	ZWILCH	0.044117647	Missense_L569V, Silent
15	exm1190716	[A/G]	UNC45A	0.010989011	Missense_M249I, Missense_M264I
15	exm1156124	[A/G]	TP53BP1	0.045454545	Missense_P1341S, Missense_P1341S, Missense_P1336S
15	exm1146914	[A/G]	AQR	0.045454545	Missense_P1481L
15	exm1160701	[T/G]	ATP8B4	0.028571429	Missense_P371H
15	exm1147780	[G/C]	FSIP1	0.042105263	Missense_P541A
15	exm1157351	[G/C]	CASC4	0.041501976	Missense_Q113H, Missense_Q113H
15	exm1164516	[A/T]	MNS1	0.047619048	Missense_Q151L
15	exm1191113	[T/C]	VPS33B	0.015151515	Missense_R107Q
15	exm1192792	[A/G]	LRRC28	0.045454545	Missense_R109H
15	exm1158689	[A/G]	DUOX1	0.028571429	Missense_R1481Q, Missense_R1481Q
15	exm1181151	[T/C]	ADAMTS7	0.045454545	Missense_R218H
15	exm1182530	[A/G]	IL16	0.035714286	Missense_R319H, Missense_R319H
15	exm1153234	[A/G]	PLA2G4D	0.005546956	Missense_R333W
15	exm1183163	[A/G]	FAM154B	0.047619048	Missense_R389H
15	exm1186633	[A/G]	ACAN	0.027472527	Missense_R394Q, Missense_R394Q
15	exm1173050	[A/G]	PAQR5	0.045454545	Missense_S11N, Missense_S11N
15	exm1171891	[A/G]	AAGAB	0.003611971	Missense_S220P
15	exm1176284	[A/G]	STRA6	0.024242424	Missense_S58L, Missense_S73L, Missense_S95L, Missense_S58L, Missense_S58L, Missense_S58L, Missense_S97L, Missense_S58L
15	exm1184631	[A/G]	ZNF592	0.046800826	Missense_S926N
15	exm1173024	[A/G]	GLCE	0.024509804	Missense_T453A
15	exm1148275	[T/C]	BUB1B	0.027667984	Missense_T648I
15	exm1172534	[A/G]	ITGA11	0.042105263	Missense_T960I
15	exm1185057	[A/G]	SLC28A1	0.035714286	Missense_V189I
15	exm1188412	[T/C]	PLIN1	0.035714286	Missense_V272M, Missense_V272M
15	exm1178993	[T/A]	FBXO22, FBXO22-AS1	0.030701754	Missense_X404Y, Silent, Silent
15	exm1153448	[T/C]	PLA2G4F	0.008791209	Silent, Missense_V247M
16	exm1229096	[T/C]	KIAA0556	0.035714286	Missense_A1240V
16	exm1200654	[T/C]	CACNA1H	0.044117647	Missense_A1942V, Missense_A1936V
16	exm1198320	[T/C]	WDR24	0.047619048	Missense_A390T
16	exm1217326	[T/C]	CIITA	0.018181818	Missense_A506V
16	exm1244992	[T/C]	CNGB1	0.020979021	Missense_D402N
16	exm1243334	[G/C]	CPNE2	0.035714286	Missense_D82E
16	exm1259888	[C/G]	KARS	0.032967033	Missense_E120Q, Missense_E92Q
16	exm1216939	[T/C]	EMP2	0.047619048	Missense_E121K

16	exm1227991	[A/G]	AQP8	0.045454545	Missense_E150K
16	exm1261087	[A/T]	CENPN	0.022727273	Missense_E84D, Missense_E84D, Missense_E84D
16	exm1234219	[A/G]	PHKG2	0.049122807	Missense_G86S, Missense_G86S
16	exm1202974	[T/C]	CRAMP1L	0.045454545	Missense_I1183T
16	exm1246300	[A/C]	CDH11	0.006993007	Missense_I433M
16	exm1256594	[T/C]	PKD1L3	0.029411765	Missense_K274E
16	exm1263840	[A/G]	DNAAF1	0.017404938	Missense_K393R
16	exm1224564	[T/C]	ZP2	0.013986014	Missense_M133V
16	exm1200229	[A/G]	CACNA1H	0.043956044	Missense_M313V, Missense_M313V
16	exm1267532	[T/C]	ZNF469	0.010989011	Missense_P1668L
16	exm1196373	[A/G]	TMEM8A	0.015151515	Missense_P201S
16	exm1213609	[A/G]	NMRAL1	0.020979021	Missense_P252L
16	exm1220429	[T/C]	ABCC1	0.043956044	Missense_R1066W, Missense_R1007W, Missense_R951W, Missense_R1010W, Missense_R1066W
16	exm1200424	[A/G]	CACNA1H	0.047385621	Missense_R1069Q, Missense_R1069Q
16	exm1221023	[T/C]	XYLT1	0.000333	Missense_R147Q
16	exm1250942	[T/C]	DPEP3	0.047619048	Missense_R154K, Missense_R154K
16	exm1259635	[G/C]	TMEM231	0.024509804	Missense_R266T, Missense_R237T, Missense_R121T
16	exm1263012	[A/G]	MLYCD	0.035714286	Missense_R392Q
16	exm1247857	[T/C]	KIAA0895L	0.026923077	Missense_R459Q
16	exm1254754	[A/G]	HYDIN	0.026923077	Missense_R4952W
16	exm1233884	[A/G]	SRCAP	0.045454545	Missense_R966Q
16	exm1262654	[G/C]	SDR42E1	0.010882822	Missense_S10T
16	exm1265329	[A/C]	CRISPLD2	0.043956044	Missense_S144R
16	exm1261567	[T/G]	PKD1L2	0.017857143	Missense_S1665Y
16	exm1247524	[A/C]	CES4A	0.035714286	Missense_S258R, Missense_S160R, Missense_S164R
16	exm1251225	[A/T]	NFATC3	0.045454545	Missense_S269T, Missense_S269T, Missense_S269T
16	exm1236325	[A/G]	ITGAX	0.029411765	Missense_T123A
16	exm1243998	[A/G]	GPR114	0.017857143	Missense_T20A
16	exm1207604	[A/C]	CCNF	0.032967033	Missense_T327K
16	exm1247343	[T/C]	CES2	0.012820513	Missense_T336M, Missense_T336M, Silent
16	exm1215572	[A/G]	NAGPA	0.025641026	Missense_T465I
16	exm1268951	[A/G]	PIEZO1	0.045454545	Missense_T563M
16	exm1225201	[T/C]	VWA3A	0.022242889	Missense_T657I
16	exm1256018	[T/C]	PHLPP2	0.045454545	Missense_V1282I
16	exm1252046	[A/G]	CDH3	0.032967033	Missense_V561M
16	exm1210668	[A/T]	MEFV	0.045454545	Silent, Missense_D424E
16	exm1199791	[C/G]	LMF1	0.044117647	Silent, Missense_P562R, Silent
16	exm1199880	[T/C]	LMF1	0.047619048	Silent, Missense_R230Q, Silent
17	exm1301651	[A/G]	TBC1D28	0.026315789	Missense_A105V
17	exm1294762	[T/C]	MYH2	0.024242424	Missense_A1444T, Missense_A1444T
17	exm1280149	[A/G]	SPNS3	0.047619048	Missense_A269T

17	exm1290905	[T/G]	ALOXE3	0.047619048	Missense_A282D, Missense_A150D
17	exm1350119	[A/G]	SLC39A11	0.007936508	Missense_A287V, Missense_A280V
17	exm1273436	[T/C]	GEMIN4	0.037409701	Missense_D929N
17	exm1283034	[T/C]	ZNF232	0.018181818	Missense_E36K
17	exm1314605	[T/C]	SYNRG	0.018181818	Missense_E717K, Missense_E717K, Missense_E716K, Missense_E795K, Missense_E717K, Missense_E717K, Missense_E634K
17	exm1353827	[G/C]	GGA3	0.047619048	Missense_E97Q, Silent, Missense_E186Q, Missense_E147Q, Missense_E219Q
17	exm1294342	[T/C]	MYH4	0.040559441	Missense_G256D
17	exm1363303	[A/G]	GAA	0.047619048	Missense_G576S, Missense_G576S, Missense_G576S
17	exm1338149	[T/C]	TOM1L1	0.045454545	Missense_L348F
17	exm1349475	[A/G]	ABCA10	0.029411765	Missense_L663S
17	exm1361017	[T/C]	DNAH17	0.04743083	Missense_M1986V
17	exm1296641	[T/C]	COX10	0.034965035	Missense_P104L
17	exm1317248	[T/C]	ERBB2	0.045454545	Missense_P1177L, Missense_P1207L
17	exm1365385	[A/G]	AATK	0.045454545	Missense_P1192S, Missense_P1089S
17	exm1369369	[A/G]	FASN	0.027777778	Missense_P617L
17	exm1303396	[A/G]	ALDH3A1	0.038461538	Missense_P79L, Missense_P79L, Missense_P79L
17	exm1369510	[T/G]	CCDC57	0.040959041	Missense_Q810K
17	exm1321241	[A/C]	KRT31	0.021978022	Missense_R208L
17	exm1286100	[A/G]	DVL2	0.028571429	Missense_R237W
17	exm1342903	[A/G]	BRIP1	0.018181818	Missense_R264W
17	exm1327656	[T/C]	G6PC3	0.028571429	Missense_R274C, Silent, Silent
17	exm1284328	[T/C]	WSCD1	0.035714286	Missense_R303W
17	exm1295950	[A/G]	DNAH9	0.047619048	Missense_R3726Q, Missense_R38Q
17	exm1331597	[A/G]	GOSR2	0.046034203	Missense_R67K, Missense_R67K, Missense_R67K
17	exm1304297	[A/G]	KCNJ12, KCNJ18	0.040959041	Missense_R6Q, Missense_R6Q
17	exm1354940	[T/C]	RECQL5	0.021978022	Missense_R770Q
17	exm1311887	[T/C]	UNC45B	0.031857032	Missense_R776W, Missense_R778W
17	exm1321356	[A/T]	KRT37	0.033333333	Missense_S73C
17	exm1295567	[A/G]	DNAH9	0.031620553	Missense_T1221A
17	exm1322017	[A/G]	KRT19	0.036119711	Missense_T327M
17	exm1337873	[T/C]	UTP18	0.038461538	Missense_T480I
17	exm1358363	[T/C]	AANAT	0.028571429	Missense_T76I, Missense_T31I
17	exm1356970	[A/G]	EVPL	0.034965035	Missense_T835I
17	exm1326778	[C/G]	NBR1	0.016640867	Missense_V182L, Missense_V182L, Missense_V182L
17	exm1364681	[A/G]	RNF213, LOC100294362	0.036363636	Missense_V4453I, Silent
17	exm1290479	[A/G]	GUCY2D	0.038461538	Missense_V662M
17	exm1363356	[A/G]	GAA	0.002262443	Missense_V780I, Missense_V780I, Missense_V780I
17	exm1345904	[T/C]	TEX2	0.038461538	Missense_V881M
17	exm1296979	[A/T]	FAM18B2-CDRT4, CDRT4	0.013986014	Silent, Silent, Missense_N163Y
17	exm1288528	[A/G]	SHBG	0.043956044	Silent, Silent, Synonymous_K286K, Missense_D356N, Missense_D241N, Missense_D338N
18	exm1378989	[A/G]	LAMA3	0.006993007	Missense_A2146T, Missense_A2090T, Missense_A481T, Missense_A537T

18	exm1392259	[A/G]	RTTN	0.024242424	Missense_A240V
18	exm1379174	[T/C]	TTC39C	0.024509804	Missense_A388V, Missense_A449V
18	exm1378848	[T/G]	LAMA3	0.011904762	Missense_D1372Y, Missense_D1372Y
18	exm1371494	[A/G]	CLUL1	0.001262626	Missense_E173K, Missense_E173K
18	exm1371832	[C/G]	METTL4	0.045454545	Missense_E239Q
18	exm1387358	[A/G]	SMAD4	0.026923077	Missense_E374K
18	exm1377011	[C/G]	MC5R	0.024242424	Missense_F209L
18	exm1381158	[A/G]	DSG2	0.018181818	Missense_H74R
18	exm1374780	[A/G]	ANKRD12	0.001262626	Missense_K906R, Missense_K883R, Missense_K883R
18	exm1378769	[T/C]	LAMA3	0.031857032	Missense_L937F, Missense_L937F
18	exm1378441	[T/C]	NPC1	0.040559441	Missense_N961S
18	exm1374337	[T/C]	CCDC165	0.024242424	Missense_R253W
18	exm1383557	[A/G]	TPGS2	0.034502262	Missense_R47C
18	exm1381499	[T/C]	TRAPPC8	0.044117647	Missense_R609H
18	exm1382923	[A/G]	SLC39A6	0.049773756	Missense_R752C
18	exm1385694	[A/G]	KATNAL2	0.018181818	Missense_R85H
18	exm1381420	[G/C]	TRAPPC8	0.006993007	Missense_T1223R
18	exm1382877	[A/G]	C18orf21	0.027472527	Missense_T44A, Missense_T44A, Silent, Missense_T132A
18	exm1381205	[A/G]	DSG2	0.027634131	Missense_V515I
18	exm1375025	[A/G]	RALBP1	0.030701754	Missense_V625I
18	exm1394601	[C/G]	NFATC1	0.019230769	Silent, Missense_K398N, Missense_K398N, Missense_K385N, Missense_K385N
18	exm1388566	[G/C]	LOC100505549, ATP8B1	0.020979021	Silent, Missense_T1242S
19	exm1420350	[T/C]	MUC16	0.013931889	Missense_A12925T
19	exm1422477	[A/G]	OR7G3	0.035714286	Missense_A237V
19	exm1404924	[A/G]	ZNF556	0.020639835	Missense_A248T
19	exm1396451	[T/C]	POLRMT	0.013986014	Missense_D1085N
19	exm1427412	[A/G]	LDLR	0.036119711	Missense_D168N, Silent, Missense_D127N, Silent, Missense_D47N, Missense_D168N
19	exm1401343	[G/C]	MBD3	0.032967033	Missense_E275D
19	exm1426542	[G/C]	SLC44A2	0.024509804	Missense_E550Q, Missense_E552Q
19	exm1430165	[C/G]	ZNF20, ZNF625-ZNF20	0.036119711	Missense_F292L, Silent, Missense_F289L
19	exm1427443	[A/G]	LDLR	0.033333333	Missense_G324S, Missense_G156S, Missense_G283S, Missense_G197S, Missense_G203S, Missense_G324S
19	exm1422969	[T/A]	ZNF559-ZNF177, ZNF177	0.029411765	Missense_I295F, Silent, Missense_I295F, Missense_I455F
19	exm1415176	[A/G]	EMR1	0.044117647	Missense_I487V, Missense_I398V, Missense_I539V, Missense_I539V, Missense_I362V
19	exm1422878	[A/T]	ZNF559, ZNF559-ZNF177	0.027568922	Missense_N364I,Silent, Missense_N258I, Silent, Silent, Missense_N300I, Silent, Silent, Silent, Silent
19	exm1428643	[T/G]	RGL3	0.049113876	Missense_P162H, Missense_P162H
19	exm1397678	[T/C]	ELANE	0.033333333	Missense_P257L
19	exm1403544	[A/G]	JSRP1	0.047619048	Missense_P267S
19	exm1414494	[T/G]	C3	0.018181818	Missense_P836T
19	exm1409449	[A/C]	PLIN4	0.032967033	Missense_R1208M
19	exm1408191	[A/G]	CREB3L3	0.04747162	Missense_R392Q
19	exm1409319	[T/C]	HDGFRP2	0.032967033	Missense_T50I, Missense_T50I

19	exm1423686	[T/C]	COL5A3	0.015151515	Missense_V1691I
19	exm1415181	[A/G]	EMR1	0.014705882	Missense_V537I, Missense_V448I, Missense_V589I, Missense_V589I, Missense_V412I
19	exm1415213	[G/C]	EMR1	0.021708683	Missense_V672L, Missense_V583L, Missense_V659L, Missense_V724L, Missense_V547L
1	exm101053	[T/C]	LCE5A	0.034965035	Nonsense_R79X
12	exm1022625	[G/C]	GLIPR1L2	0.027472527	Nonsense_Y144X
13	exm1082947	[T/G]	UPF3A	0.038461538	Nonsense_E258X, Nonsense_E291X
15	exm1177922	[A/G]	MAN2C1	0.045454545	Nonsense_R878X, Nonsense_R878X, Nonsense_R895X, Nonsense_R779X
17	exm1312366	[A/G]	SLFN13	0.049773756	Nonsense_R647X
17	exm1352015	[A/C]	C17orf77	0.044117647	Nonsense_C207X
1	exm-rs984222	[C/G]	TBX15	0.020979021	Silent
1	exm-rs1342038	[A/G]	LOC100506023	0.024509804	Silent
1	exm-rs1023252	[T/G]	CLCN6	0.025641026	Silent
2	exm-rs1351164	[T/C]	DIRC3	0.025641026	Silent
2	exm-rs6732434	[A/G]	PPP1R1C	0.035714286	Silent
2	exm-rs17027258	[A/G]	SLC9A4	0.043601651	Silent
2	exm-rs41464348	[A/G]	LTBP1	0.013986014	Silent, Silent, Silent, Silent, Silent
3	exm-rs6439334	[A/G]	CPNE4	0.045454545	Silent
3	exm-rs4370013	[A/T]	CNTN4	0.019766611	Silent, Silent
3	exm-rs10935120	[A/G]	CEP63	0.010989011	Silent, Silent, Silent, Silent
4	exm-rs2273	[T/C]	SDAD1	0.033333333	Silent
4	exm-rs1391099	[A/G]	INPP4B	0.049773756	Silent, Silent
5	exm-rs26232	[T/C]	C5orf30	0.043956044	Silent
5	exm-rs31489	[A/C]	CLPTM1L	0.044547644	Silent
6	exm-rs9276431	[T/C]	HLA-DQA2	0.004545455	Silent
6	exm-rs2071556	[T/G]	HLA-DMB	0.014705882	Silent
6	exm-rs887466	[A/G]	PSORS1C3	0.015151515	Silent
6	exm-rs2213568	[A/C]	HLA-DQA2	0.027777778	Silent
6	exm-rs2074470	[A/G]	OR11A1	0.028571429	Silent
6	exm-rs2242668	[T/C]	LSM2	0.028571429	Silent
6	exm-rs6908425	[T/C]	CDKAL1	0.038461538	Silent
6	exm-rs444921	[T/C]	SKIV2L	0.047385621	Silent
6	exm-rs2844775	[A/G]	TRIM26	0.006993007	Silent, Silent
6	exm-rs3130383	[A/C]	TRIM26	0.008333333	Silent, Silent
6	exm-rs8321	[A/C]	ZNRD1	0.020979021	Silent, Silent
6	exm-rs9262113	[A/G]	PRR3	0.027472527	Silent, Silent
6	exm-rs9487094	[A/G]	PPIL6	0.027472527	Silent, Silent
6	exm-rs3132672	[A/C]	TRIM26	0.027777778	Silent, Silent
6	exm-rs4148871	[A/G]	TAP2	0.040090344	Silent, Silent
6	exm-rs6916921	[T/C]	NFKBIL1	0.026923077	Silent, Silent, Silent, Silent
6	exm-rs707939	[A/C]	MSH5, MSH5-SAPCD1	0.004662005	Silent, Silent, Silent, Silent, Silent
6	exm-rs620202	[T/G]	BRD2	0.027472527	Silent, Silent, Silent, Silent, Silent
6	exm-rs485502	[T/C]	BRD2	0.035714286	Silent, Silent, Silent, Silent, Silent

7	exm-rs730497	[A/G]	GCK	0.012820513	Silent
7	exm-rs864745	[T/C]	JAZF1	0.049773756	Silent
7	exm-rs10256972	[A/C]	C7orf50	0.043956044	Silent, Silent, Silent
8	exm-rs7009183	[A/G]	LOC100616530	0.042986425	Silent, Silent,S ilent, Silent, Silent, Silent, Silent, Silent, Silent
9	exm-rs10491539	[T/G]	SH3GL2	0.011363636	Silent
9	exm-rs17584499	[T/C]	PTPRD	0.047619048	Silent
10	exm-rs7085433	[A/G]	TIMM23	0.031991744	Silent
10	exm-rs1913517	[A/G]	WDFY4, LRRC18	0.04747162	Silent, Silent
11	exm-rs7926971	[A/G]	TEAD1	0.028101929	Silent
12	exm-rs2970818	[A/T]	C12orf4	0.018059856	Silent
12	exm-rs10846934	[T/C]	TMEM132B	0.018942963	Silent
12	exm-rs1491942	[G/C]	LRRK2	0.027472527	Silent
12	exm-rs12579350	[A/G]	ANO2	0.035947712	Silent
12	exm-rs7134594	[T/C]	MMAB	0.040559441	Silent, Silent
12	exm1036101	[T/G]	TCHP	0.045454545	Silent, Silent
14	exm-rs7140150	[T/C]	FRMD6	0.019230769	Silent
14	exm-rs7159841	[T/C]	MDGA2	0.033841159	Silent
15	exm-rs4775785	[T/C]	SHC4	0.047619048	Silent
15	exm-rs6494537	[T/C]	DENND4A	0.034965035	Silent, Silent
15	exm-rs12440440	[A/G]	RYR3	0.042744021	Silent, Silent
15	exm-rs1378942	[A/C]	CSK	0.044117647	Silent, Silent
15	exm-rs886144	[T/C]	SV2B	0.044117647	Silent, Silent
15	exm-rs12915189	[A/G]	CRTC3	0.047619048	Silent, Silent
15	exm-rs8043440	[T/C]	GABRB3	0.047619048	Silent, Silent
16	exm-rs6564869	[A/C]	GAN	0.035714286	Silent
17	exm-rs2589133	[A/G]	RPTOR	0.027472527	Silent, Silent
19	exm1421853	[T/C]	MUC16	0.032967033	Silent
19	exm1431071	[C/G]	MAN2B1	0.035714286	Silent, Silent
19	exm-rs2279008	[T/C]	MYO9B	0.044117647	Silent, Silent
20	exm-rs487656	[A/G]	LOC284757	0.043601651	Silent
21	exm-rs2826891	[T/C]	NCAM2	0.001998002	Silent
21	exm-rs7275212	[A/T]	ERG	0.045454545	Silent, Silent, Silent, Silent, Silent, Silent, Silent
22	exm-rs139553	[T/C]	MEI1	0.045796309	Silent
Y	exm-rs9341313	[T/G]	EIF1AY	0.018181818	Silent
1	exm131743	[T/C]	HMCN1, MIR548F1	0.031991744	Synonymous_A4302A, Silent
1	exm-rs1142287	[T/C]	SCAMP3	0.032868733	Synonymous_G126G, Synonymous_G100G
11	exm-rs4453265	[T/C]	C2CD3	0.047385621	Synonymous_V1641V
12	exm1041028	[T/C]	RNFT2	0.017857143	Synonymous_L183L, Synonymous_L183L
12	exm1043795	[T/C]	ACADS	0.043956044	Synonymous_N120N
12	exm1051188	[T/C]	PIWIL1	0.034965035	Synonymous_A26A, Synonymous_A26A
13	exm1068030	[A/G]	ESD	0.015151515	Synonymous_I157I
16	exm1215196	[A/G]	PPL	0.038461538	Synonymous_A826A

16	exm1244602	[T/C]	KATNB1	0.033333333	Synonymous_D410D
16	exm1210664	[T/C]	MEFV	0.032967033	Synonymous_L590L, Missense_D438N
17	exm1279218	[A/G]	ATP2A3	0.031857032	Synonymous_A632A, Synonymous_A632A, Synonymous_A632A, Synonymous_A632A, Synonymous_A632A, Synonymous_A632A, Synonymous_A632A

**PRCC vs. normalrenal tissue; Fisher's exact test. Abbreviations: PRCC, Papillaryrenal cell carcinoma; Chr, chromosome; SNP, single nucleotidepolymorphism.

Table 4. Gene Ontology (GO) functional enrichment and Kyoto Encyclopedia of Genes and Genomes (KEGG) pathway analyses of the 287 missense mutated genes of Papillary renal cell carcinoma ($p < 0.05$) detected by Human Exome BeadChip technology

Category	Cluster	Term	Gene Count	%	*P* Value	Genes
GOTERM_BP_FAT	Cell adhesion	GO:0007155~cell adhesion	65	6.220095694	1.78E-05	MTSS1, AEBP1, NRP1, CLSTN2, CLSTN1, PCDHA1, PCDHGA1, CLEC4A, COL12A1, SPON1, RET, PCDHB5, CNTNAP5, CDHR1, COL22A1, MYH9, SSPO, GPR98, SIGLEC1, SIGLEC6, HAS1, CPXM1, RELN, CNTN4, COL24A1, DST, ADAMTS13, ITGA11, CRNN, CDH3, DCHS1, ITGAM, LAMB3, COL7A1, SORBS1, AGGF1, ITGAX, FAT4, FAT1, COL27A1, ACAN, COL6A1, LPP, PPFIBP1, HSPG2, COL15A1, PCDH15, NID1, COL5A3, COL4A6, VWF, CASS4, COL19A1, LAMA3, DSG2, EMR1, ERBB2IP, CDH17, FREM2, TMEM8A, LAMA5, FREM1, MUC5B, CDH11, MUC16
GOTERM_BP_FAT		GO:0022610~biological adhesion	65	6.220095694	1.90E-05	MTSS1, AEBP1, NRP1, CLSTN2, CLSTN1, PCDHA1, PCDHGA1, CLEC4A, COL12A1, SPON1, RET, PCDHB5, CNTNAP5, CDHR1, COL22A1, MYH9, SSPO, GPR98, SIGLEC1, SIGLEC6, HAS1, CPXM1, RELN, CNTN4, COL24A1, DST, ADAMTS13, ITGA11, CRNN, CDH3, DCHS1, ITGAM, LAMB3, COL7A1, SORBS1, AGGF1, ITGAX, FAT4, FAT1, COL27A1, ACAN, COL6A1, LPP, PPFIBP1, HSPG2, COL15A1, PCDH15, NID1, COL5A3, COL4A6, VWF, CASS4, COL19A1, LAMA3, DSG2, EMR1, ERBB2IP, CDH17, FREM2, TMEM8A, LAMA5, FREM1, MUC5B, CDH11, MUC16
GOTERM_BP_FAT		GO:0007156~homophilic cell adhesion	16	1.531100478	0.004375914	RET, PCDHB5, CLSTN2, CDHR1, CLSTN1, PCDH15, PCDHA1, CDH3, DCHS1, PCDHGA1, DSG2, FAT4, FREM2, CDH17, FAT1, CDH11
GOTERM_BP_FAT		GO:0016337~cell-cell adhesion	24	2.296650718	0.024451853	RET, CLSTN2, PCDHB5, CDHR1, CLSTN1, PCDH15, CRNN, PCDHA1, MYH9, CDH3, ITGAM, DCHS1, GPR98, PCDHGA1, SIGLEC1, COL19A1, DSG2, FAT4, CDH17, FREM2, FAT1, ACAN, CNTN4, CDH11
GOTERM_BP_FAT	Microtubule-based movement	GO:0007018~microtubule-based movement	14	1.339712919	0.007391122	DNAH11, DNAH9, OPA1, DNAH12, KIF11, DNAH17, BICD2, DNAH5, KIF2C, MACF1, TUBAL3, DYNC2H1, TUBB1, DST
GOTERM_BP_FAT		GO:0030705~cytoskeleton-dependent intracellular transport	8	0.765550239	0.020201062	OPA1, MACF1, MYH2, MYH4, MYH14, MYH6, MYH9, DST
GOTERM_BP_FAT		GO:0000226~microtubule cytoskeleton organization	15	1.435406699	0.026238636	RET, CEP120, KIF11, CETN3, TBCE, BRCA2, PLK1S1, MYH9, KIF2C, SASS6, MACF1, BUB1B, MAP7, TUBB1, DST
GOTERM_BP_FAT		GO:0007010~cytoskeleton organization	35	3.349282297	0.018418181	MTSS1, BMP10, CEP120, CETN3, TTN, KIF2C, MACF1, SORBS1, OBSL1, TUBB1, RET, KIF11, SPTBN5, TBCE, BRCA2, CECR2, ARHGEF17, MYH6, PLK1S1, RICTOR, MYH9, PALLD, PLCE1, SASS6, KRT19, ERBB2IP, XIRP2, LAMA5, LIMCH1, PRR5-ARHGAP8, BUB1B, MAP7, ARAP3, DST, CDC42BPB
GOTERM_BP_FAT		GO:0007017~microtubule-based process	25	2.392344498	0.004789572	DNAH11, DNAH9, DNAH12, CEP120, DNAH17, CETN3, DNAH5, KIF2C, MACF1, DYNC2H1, TUBB1, RET, KIF11, OPA1, TBCE, BRCA2, PLK1S1, MYH9, BICD2, SASS6, TUBAL3, BUB1B, MAP7, DST, MAP3K11

GOTERM_BP_FAT	Signaling pathway	GO:0007229~integrin-mediated signaling pathway	11	1.052631579	0.003945816	ADAMTS7, VAV3, ITGAX, ERBB2IP, ADAMTS13, LAMA5, ITGA11, MYH9, DST, ITGAM, ADAMDEC1
GOTERM_BP_FAT		GO:0035023~regulation of Rho protein signal transduction	15	1.435406699	7.82E-04	OBSCN, VAV3, RALBP1, PREX2, ARHGEF17, RICTOR, TTN, FARP1, MCF2L2, PLEKHG2, SYDE2, RASGRF2, TIAM1, ARAP3, KALRN
GOTERM_BP_FAT		GO:0051056~regulation of small GTPase mediated signal transduction	25	2.392344498	0.004617191	ERBB2, PREX2, RGL3, TTN, MCF2L2, PLEKHG2, TIAM1, KNDC1, OBSCN, VAV3, RALBP1, SIPA1L2, ARHGEF17, RICTOR, FARP1, PLCE1, SYDE2, RASGRF2, TBC1D28, GRTP1, C6ORF170, RELN, ARAP3, TBC1D8B, KALRN
GOTERM_BP_FAT		GO:0046578~regulation of Ras protein signal transduction	21	2.009569378	0.009082897	OBSCN, VAV3, RALBP1, ERBB2, PREX2, ARHGEF17, RICTOR, TTN, FARP1, MCF2L2, PLCE1, PLEKHG2, SYDE2, RASGRF2, TBC1D28, TIAM1, GRTP1, C6ORF170, ARAP3, TBC1D8B, KALRN
GOTERM_BP_FAT		GO:0007167~enzyme linked receptor protein signaling pathway	27	2.583732057	0.046239768	MTSS1, BMP10, FGFR4, NRP1, LTBP2, ERBB2, BDKRB2, TGFB1, SORBS1, TIAM1, GDF9, AGRN, EGF, ROS1, RET, PTPRG, SMAD4, GUCY2C, EPHA1, EPHA3, GUCY2D, EPHA5, PLCE1, ERBB2IP, NTRK2, FSHB, AKAP4
GOTERM_BP_FAT		GO:0019722~calcium-mediated signaling	6	0.574162679	0.045969671	PLCE1, MCTP2, IL8, ALMS1, NFKBIL1, MCTP1
GOTERM_BP_FAT		GO:0006468~protein amino acid phosphorylation	49	4.688995215	0.023096414	BMP10, PASK, RPS6KB2, PINK1, TTN, TGFB1, PSKH2, MAP3K5, AAK1, ROS1, IRAK2, RET, MYO3A, PHKG2, MYLK4, SRPK1, CDKL4, MAST4, HUNK, PLCE1, PROK1, RELN, LRRK2, LRRK1, EIF2AK4, KALRN, MAP3K11, FGFR4, ERBB2, STK10, C5, TRIB3, SGK223, TTBK2, EGF, AATK, OBSCN, FSCB, ATR, OXSR1, GUCY2C, EPHA1, EPHA3, GUCY2D, EPHA5, MAPK12, NTRK2, GRK6, CDC42BPB
GOTERM_BP_FAT	Cell cycle process	GO:0022402~cell cycle process	49	4.688995215	0.001052892	MLH3, TTN, TGFB1, KIF2C, DDX11, INCENP, PIWIL3, C11ORF82, TUBB1, ASPM, KIF11, CGRRF1, SGOL2, CCNF, POLE, PLK1S1, MYH9, NCAPD2, REC8, SASS6, PPM1D, FANCD2, BUB1B, HORMAD2, NUP43, DST, MAP3K11, CEP120, TIPIN, CETN3, KIAA1009, PLAGL1, PRUNE2, PSMF1, MACF1, MNS1, GFI1, ZWILCH, NFATC1, IL8, CENPF, BRCA2, TP73, RGS14, PSMB9, CCNB3, TEX15, MAPK12, APBB1
GOTERM_BP_FAT		GO:0030203~glycosaminoglycan metabolic process	10	0.956937799	0.002400935	HYAL2, GCNT2, SPOCK3, XYLT1, HAS1, GALNT5, HEXB, ITIH5, DSE, GLCE
GOTERM_BP_FAT		GO:0007049~cell cycle	60	5.741626794	0.003955172	STEAP3, MLH3, TTN, TGFB1, KIF2C, DDX11, INCENP, PIWIL3, C11ORF82, TUBB1, ASPM, KIF11, CGRRF1, SGOL2, POLE, CCNF, MCM2, PLK1S1, MYH9, AHR, NCAPD2, PPM1D, REC8, SASS6, EP300, RIF1, FANCD2, PRR5-ARHGAP8, BUB1B, TMPRSS11A, HORMAD2, NUP43, DST, MAP3K11, CEP120, CETN3, TIPIN, KIAA1009, PLAGL1, PSMF1, PRUNE2, MACF1, HJURP, MNS1, GFI1, ZWILCH, NFATC1, CKAP2, IL8, CENPF, BRCA2, ATR, RGS14, TP73, PSMB9, CCNB3, TEX15, ERBB2IP, MAPK12, APBB1
GOTERM_BP_FAT		GO:0070192~chromosome organization involved in meiosis	4	0.38277512	0.029295159	REC8, TEX15, FANCD2, MLH3
GOTERM_BP_FAT		GO:0000279~M phase	29	2.775119617	0.010713242	CEP120, TIPIN, CETN3, MLH3, TTN, KIAA1009, KIF2C, DDX11, INCENP, MNS1, PIWIL3, ZWILCH, TUBB1, ASPM, KIF11, SGOL2, CCNF, BRCA2, CENPF, MYH9, RGS14, NCAPD2, REC8, CCNB3, TEX15, FANCD2, BUB1B, HORMAD2, NUP43
GOTERM_BP_FAT		GO:0007059~chromosome segregation	10	0.956937799	0.028905796	REC8, DDX11, HJURP, SGOL2, INCENP, CENPF, TTN, NUP43, SRPK1, NCAPD2
GOTERM_BP_FAT		GO:0045005~maintenance of fidelity during DNA-dependent DNA replication	3	0.28708134	0.025738663	TIPIN, BRCA2, WRN
GOTERM_BP_FAT		GO:0022403~cell cycle phase	35	3.349282297	0.008864905	CEP120, CETN3, TIPIN, MLH3, TTN, KIAA1009, PRUNE2, KIF2C, DDX11, INCENP, MNS1, PIWIL3, GFI1, ZWILCH, TUBB1, ASPM, NFATC1, KIF11, SGOL2, CCNF, POLE, CENPF, BRCA2, MYH9, RGS14, NCAPD2, CCNB3, REC8, PPM1D, TEX15, FANCD2, BUB1B, HORMAD2, NUP43, MAP3K11

GOTERM_BP_FAT	Polysaccharide biosynthetic process	GO:0006024~glycosaminoglycan biosynthetic process	6	0.574162679	0.004327438	GCNT2, XYLT1, HAS1, GALNT5, DSE, GLCE
GOTERM_BP_FAT		GO:0005976~polysaccharide metabolic process	14	1.339712919	0.006372263	HYAL2, GCNT2, SPOCK3, PHKG2, GALNT5, HEXB, DSE, GLCE, XYLT1, HAS1, MGAM, GAA, ITIH5, AGL
GOTERM_BP_FAT		GO:0000271~polysaccharide biosynthetic process	8	0.765550239	0.009446334	GCNT2, XYLT1, HAS1, GALNT5, PHKG2, DSE, AGL, GLCE
GOTERM_BP_FAT		GO:0006023~aminoglycan biosynthetic process	6	0.574162679	0.006548599	GCNT2, XYLT1, HAS1, GALNT5, DSE, GLCE
GOTERM_BP_FAT		GO:0006022~aminoglycan metabolic process	10	0.956937799	0.007510441	HYAL2, GCNT2, SPOCK3, XYLT1, HAS1, GALNT5, HEXB, ITIH5, DSE, GLCE
GOTERM_BP_FAT	Tissue morphogenesis	GO:0043062~extracellular structure organization	18	1.722488038	0.006517427	RXFP1, PCDHB5, ERBB2, UTRN, HSPG2, NRD1, NID1, COL5A3, COL5A2, SPINK5, COL4A6, TNFRSF11B, COL19A1, CRISPLD2, ACAN, COL12A1, AGRN, APBB1
GOTERM_BP_FAT		GO:0030198~extracellular matrix organization	13	1.244019139	0.009627305	RXFP1, HSPG2, NID1, COL5A3, COL5A2, SPINK5, COL4A6, TNFRSF11B, COL19A1, CRISPLD2, ACAN, COL12A1, APBB1
GOTERM_BP_FAT		GO:0032989~cellular component morphogenesis	32	3.062200957	0.023088526	BMP10, PLXNA3, SHROOM2, NRP1, COX10, ERBB2, TTN, TGFB1, MACF1, DYNC2H1, OBSL1, GDF9, ROBO3, NFATC1, OPA1, C2CD3, TBCE, ALMS1, MYH6, MYH9, SLIT2, KRT19, ERBB2IP, LAMA5, PRICKLE2, RELN, CNTN4, MAP7, APBB1, DST, CDC42BPB, KALRN
GOTERM_BP_FAT		GO:0048729~tissue morphogenesis	17	1.626794258	0.032413281	DVL2, BMP10, RET, C2CD3, SMAD4, MYH6, NR4A3, TTN, GLI3, TCF7L1, SLIT2, FZD6, MACF1, FREM2, LAMA5, GAA, KLK14
GOTERM_BP_FAT		GO:0043954~cellular component maintenance	8	0.765550239	2.54E-04	IQCB1, SHROOM2, CDHR1, PCDH15, CNGB1, ACAD11, USH2A, GPR98
GOTERM_BP_FAT		GO:0048496~maintenance of organ identity	4	0.38277512	5.89E-04	IQCB1, ACAD11, USH2A, GPR98
GOTERM_BP_FAT	Maintenance of organ identity	GO:0050953~sensory perception of light stimulus	20	1.913875598	0.023223977	IQCB1, OPA1, MYO3A, BBS9, CDHR1, RP2, RP1L1, ALMS1, PCDH15, CNGB1, CDH3, CDS1, GPR98, GUCY2D, EYA4, EYS, HMCN1, IMPG1, ACAD11, USH2A
GOTERM_BP_FAT		GO:0007601~visual perception	20	1.913875598	0.023223977	IQCB1, OPA1, MYO3A, BBS9, CDHR1, RP2, RP1L1, ALMS1, PCDH15, CNGB1, CDH3, CDS1, GPR98, GUCY2D, EYA4, EYS, HMCN1, IMPG1, ACAD11, USH2A
GOTERM_BP_FAT		GO:0045494~photoreceptor cell maintenance	7	0.669856459	6.29E-04	IQCB1, CDHR1, PCDH15, CNGB1, ACAD11, USH2A, GPR98
GOTERM_BP_FAT		GO:0050954~sensory perception of mechanical stimulus	11	1.052631579	0.0491677	KCNQ4, MYO3A, CHRNA9, MCOLN3, HEXB, TRPA1, GJB3, ALMS1, PCDH15, USH2A, GPR98

GOTERM_BP_FAT	Muscle cell development, differentiation	GO:0045214~sarcomere organization	4	0.38277512	0.023449715	BMP10, KRT19, MYH6, TTN
GOTERM_BP_FAT		GO:0030239~myofibril assembly	5	0.4784689	0.023617794	BMP10, KRT19, OBSL1, MYH6, TTN
GOTERM_BP_FAT		GO:0014706~striated muscle tissue development	13	1.244019139	0.025697664	BMP10, ERBB2, UTRN, HSPG2, NRD1, MYH6, TTN, COL19A1, EP300, GAA, OBSL1, ZFPM2, AGRN
GOTERM_BP_FAT		GO:0031032~actomyosin structure organization	6	0.574162679	0.015342389	BMP10, KRT19, LIMCH1, OBSL1, MYH6, TTN
GOTERM_BP_FAT		GO:0051146~striated muscle cell differentiation	11	1.052631579	0.019053324	BMP10, KRT19, ERBB2, UTRN, CACNA1H, NRD1, OBSL1, AGRN, MYH6, MYH9, TTN
GOTERM_BP_FAT		GO:0055001~muscle cell development	9	0.861244019	0.009510235	BMP10, KRT19, ERBB2, UTRN, NRD1, OBSL1, AGRN, MYH6, TTN
GOTERM_BP_FAT		GO:0042692~muscle cell differentiation	13	1.244019139	0.028805	BMP10, ERBB2, UTRN, NRD1, MYH6, TTN, MYH9, SYNE1, KRT19, MAPK12, OBSL1, CACNA1H, AGRN
GOTERM_BP_FAT		GO:0060537~muscle tissue development	13	1.244019139	0.03581975	BMP10, ERBB2, UTRN, HSPG2, NRD1, MYH6, TTN, COL19A1, EP300, GAA, OBSL1, ZFPM2, AGRN
GOTERM_BP_FAT		GO:0030048~actin filament-based movement	5	0.4784689	0.032123528	MYH2, MYH4, MYH14, MYH6, MYH9
GOTERM_BP_FAT		GO:0055002~striated muscle cell development	9	0.861244019	0.006074436	BMP10, KRT19, ERBB2, UTRN, NRD1, OBSL1, AGRN, MYH6, TTN
GOTERM_BP_FAT		GO:0007517~muscle organ development	22	2.105263158	0.00464554	BMP10, AEBP1, ERBB2, UTRN, HSPG2, ITGA11, CENPF, NRD1, MYH6, TTN, EP300, COL19A1, MAPK12, NEB, LAMA5, GAA, CACNA1H, OBSL1, ZFPM2, AGRN, UNC45B, UNC45A
GOTERM_BP_FAT		GO:0048747~muscle fiber development	6	0.574162679	0.037333701	ERBB2, UTRN, NRD1, AGRN, MYH6, TTN
GOTERM_BP_FAT		GO:0007507~heart development	19	1.818181818	0.040567691	DVL2, BMP10, NRP1, C2CD3, ERBB2, HSPG2, OXTR, MYH6, TTN, GLI3, PLCE1, EP300, SALL4, GAA, OBSL1, ZFPM2, ADAM19, NFATC3, NFATC1
GOTERM_BP_FAT	Negative regulation	GO:0050860~negative regulation of T cell receptor signaling pathway	3	0.28708134	0.025738663	ELF1, CBLB, UBASH3A
GOTERM_BP_FAT		GO:0050858~negative regulation of antigen receptor-mediated signaling pathway	3	0.28708134	0.025738663	ELF1, CBLB, UBASH3A
GOTERM_BP_FAT		GO:0010596~negative regulation of endothelial cell migration	4	0.38277512	0.035834358	BMP10, AGTR2, DLL4, TGFB1
GOTERM_BP_FAT		GO:0045792~negative regulation of cell size	11	1.052631579	0.039161459	RTN4, BMP10, PLXNA3, AGTR2, NRP1, CGRRF1, SMAD4, GDF9, APBB1, TP73, TGFB1
GOTERM_BP_FAT		GO:0030308~negative regulation of cell growth	11	1.052631579	0.025196073	RTN4, BMP10, PLXNA3, AGTR2, NRP1, CGRRF1, SMAD4, GDF9, APBB1, TP73, TGFB1
GOTERM_BP_FAT	Cell death	GO:0008219~cell death	51	4.880382775	0.036510953	STEAP3, RTN4, TSPO, FASTKD1, TGFB1, MAGED1, TNFRSF11B, MAP3K5, TIAM1, CLUL1, C11ORF82, CASP1, API5, MAGI3, OPA1, GZMA, PTPRH, SCN2A, CECR2, ARHGEF17, AHR, EP300, RASGRF2, ZFYVE27, ZFYVE26, SH3KBP1, BUB1B, KALRN, MAP3K11, C5, TRIB3, PRUNE2, PLEKHG2, ATN1, TTBK2, TRAF5, HIP1, AATK, CKAP2, OBSCN, CARD8, VAV3, ALMS1, CIDEA, FIG4, TP73, NFKBIL1, ATXN3, SYNE1, PARP4, APBB1
GOTERM_BP_FAT		GO:0016265~death	51	4.880382775	0.039214579	STEAP3, RTN4, TSPO, FASTKD1, TGFB1, MAGED1, TNFRSF11B, MAP3K5, TIAM1, CLUL1, C11ORF82, CASP1, API5, MAGI3, OPA1, GZMA, PTPRH, SCN2A, CECR2, ARHGEF17, AHR, EP300, RASGRF2, ZFYVE27, ZFYVE26, SH3KBP1, BUB1B, KALRN, MAP3K11, C5, TRIB3, PRUNE2, PLEKHG2, ATN1, TTBK2, TRAF5, HIP1, AATK, CKAP2, OBSCN, CARD8, VAV3, ALMS1, CIDEA, FIG4, TP73, NFKBIL1, ATXN3, SYNE1, PARP4, APBB1

GOTERM_BP_FAT	Other	GO:0009566~fertilization	10	0.956937799	0.025036283	ACR, PLCZ1, APOB, TEX15, ZP2, CD46, HEXB, UBXN8, KLK14, AKAP4
GOTERM_BP_FAT		GO:0007129~synapsis	4	0.38277512	0.029295159	REC8, TEX15, FANCD2, MLH3
KEGG_PATHWAY	KEGG pathway	hsa02010:ABC transporters	10	0.956937799	4.87E-04	ABCA10, ABCG5, TAP1, ABCC4, ABCC10, ABCC1, ABCB5, ABCA6, ABCA13, ABCB4
KEGG_PATHWAY		hsa04512:ECM-receptor interaction	14	1.339712919	5.35E-04	COL4A1, HSPG2, ITGA11, COL5A3, COL5A2, COL4A6, HMMR, VWF, LAMB3, LAMA3, LAMA5, COL6A1, RELN, AGRN
KEGG_PATHWAY		hsa04142:Lysosome	13	1.244019139	0.024611161	ARSB, AP1B1, HEXB, ASAH1, SLC11A1, NPC1, NAGPA, LAPTM5, IGF2R, GAA, CTSB, ATP6V0D2, GGA3
KEGG_PATHWAY		hsa04610:Complement and coagulation cascades	9	0.861244019	0.032655465	F11, VWF, CR2, MASP1, FGA, C3, CD46, C5, BDKRB2
KEGG_PATHWAY		hsa00630:Glyoxylate and dicarboxylate metabolism	4	0.38277512	0.044700865	MTHFD1, ACO1, HAO2, GRHPR

Abbreviations: ECM, extracellular matrix.

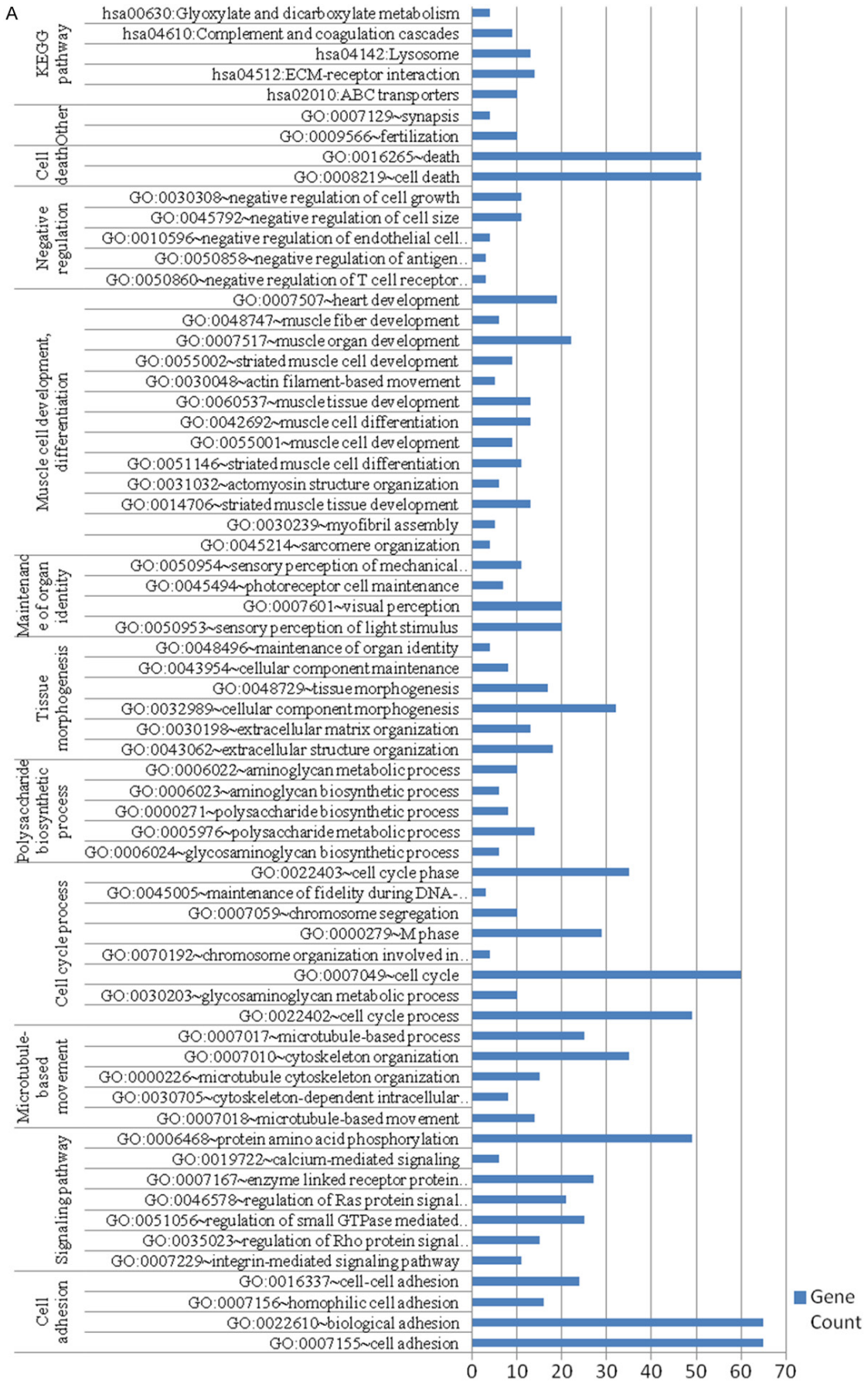
A
KEGG pathway
hsa00630:Glyoxylate and dicarboxylate metabolism
hsa04610:Complement and coagulation cascades
hsa04142:Lysosome
hsa04512:ECM-receptor interaction
hsa02010:ABC transporters
Other
GO:0007129~synapsis
GO:0009566~fertilization
Cell death
GO:0016265~death
GO:0008219~cell death
Negative regulation
GO:0030308~negative regulation of cell growth
GO:0045792~negative regulation of cell size
GO:0010596~negative regulation of endothelial cell..
GO:0050858~negative regulation of antigen..
GO:0050860~negative regulation of T cell receptor..
Muscle cell development, differentiation
GO:0007507~heart development
GO:0048747~muscle fiber development
GO:0007517~muscle organ development
GO:0055002~striated muscle cell development
GO:0030048~actin filament-based movement
GO:0060537~muscle tissue development
GO:0042692~muscle cell differentiation
GO:0055001~muscle cell development
GO:0051146~striated muscle cell differentiation
GO:0031032~actomyosin structure organization
GO:0014706~striated muscle tissue development
GO:0030239~myofibril assembly
GO:0045214~sarcomere organization
Maintenance of organ identity
GO:0050954~sensory perception of mechanical..
GO:0045494~photoreceptor cell maintenance
GO:0007601~visual perception
GO:0050953~sensory perception of light stimulus
Tissue morphogenesis
GO:0048496~maintenance of organ identity
GO:0043954~cellular component maintenance
GO:0048729~tissue morphogenesis
GO:0032989~cellular component morphogenesis
GO:0030198~extracellular matrix organization
GO:0043062~extracellular structure organization
Polysaccharide biosynthetic process
GO:0006022~aminoglycan metabolic process
GO:0006023~aminoglycan biosynthetic process
GO:0000271~polysaccharide biosynthetic process
GO:0005976~polysaccharide metabolic process
GO:0006024~glycosaminoglycan biosynthetic process
Cell cycle process
GO:0022403~cell cycle phase
GO:0045005~maintenance of fidelity during DNA-..
GO:0007059~chromosome segregation
GO:0000279~M phase
GO:0070192~chromosome organization involved in..
GO:0007049~cell cycle
GO:0030203~glycosaminoglycan metabolic process
GO:0022402~cell cycle process
Microtubule-based movement
GO:0007017~microtubule-based process
GO:0007010~cytoskeleton organization
GO:0000226~microtubule cytoskeleton organization
GO:0030705~cytoskeleton-dependent intracellular..
GO:0007018~microtubule-based movement
Signaling pathway
GO:0006468~protein amino acid phosphorylation
GO:0019722~calcium-mediated signaling
GO:0007167~enzyme linked receptor protein..
GO:0046578~regulation of Ras protein signal..
GO:0051056~regulation of small GTPase mediated..
GO:0035023~regulation of Rho protein signal..
GO:0007229~integrin-mediated signaling pathway
Cell adhesion
GO:0016337~cell-cell adhesion
GO:0007156~homophilic cell adhesion
GO:0022610~biological adhesion
GO:0007155~cell adhesion
0
10
20
30
40
50
60
70
Gene Count

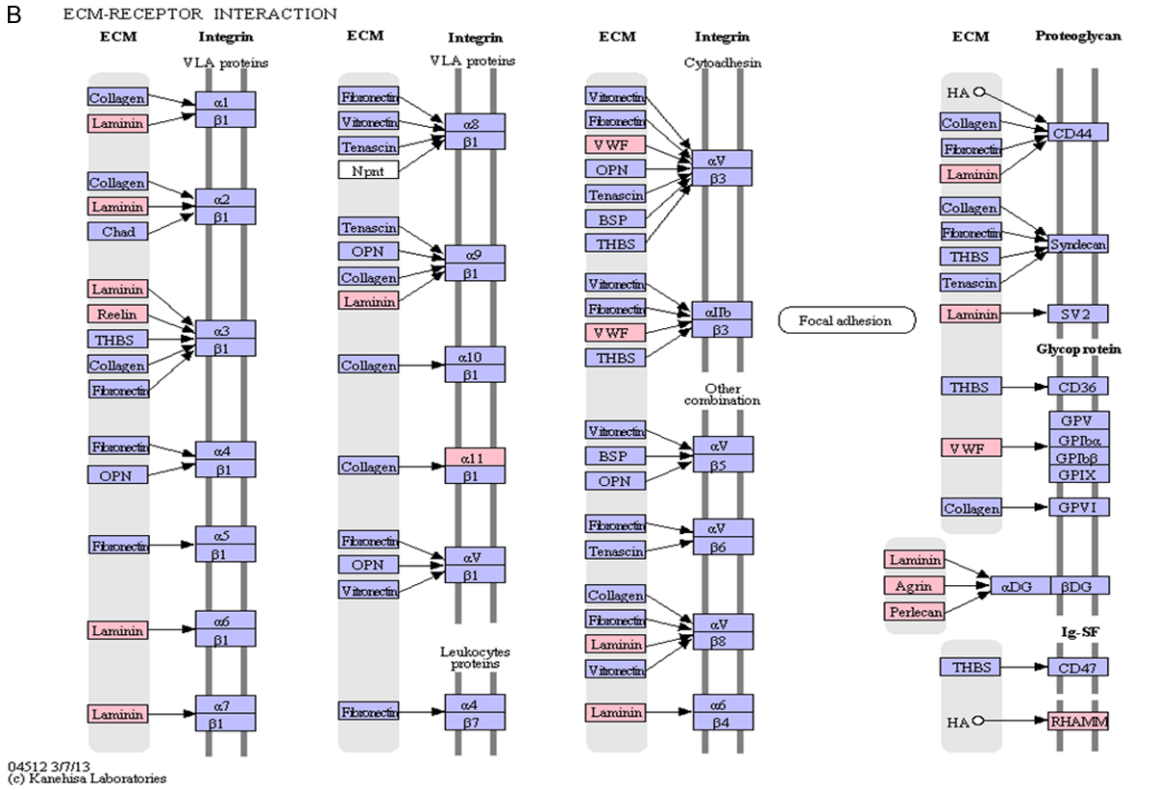

Figure 2. Functional enrichment analysis of the 211 missense-mutated genes detected by exome sequencing in PRCC. A. The related biological process categories of the 211 missense-mutated genes in CRCC. B. The extracellular matrix (ECM)-receptor interaction pathway. red genes, mutated genes in PRCC. Pathway information was generated using the Kyoto Encyclopedia of Genes and Genomes database.

sion [42-44], indicating that the frequent mutations of the collagen genes may be one of factors responsible for the development of PRCC, and that evaluating the collagen levels of PRCC patient may be useful for assessing the tumor biological behavior and prognosis.

There have reports that type 1 and 2 PRCC show more copy number changes at 17q and 9p [45-48]. Furthermore, copy number changes at 17q were more common in TNM stage 1-2 PRCC and correlated with lower stage, less lymphatic metastases, and increased survival, whereas changes at 9p conversely correlated with higher stage (TNM stage 3-4) and nuclear grade, more lymphatic metastasis, and decreased survival [45-47]. Meanwhile, amplification of chromosome 17 is another characteristic of PRCC [45, 49, 50], and changes at 17q and 9p can aid the differential diagnosis, as well as predict the prognosis in different subtypes, suggesting that genes on these chromosomes may be related to the development of type 1 or 2 PRCC. The results from exon chip analyses are consistent with previous reports in the field, with some gene exon mutations being found in specific altered chromosomal regions. For example, ERBB2 locate on 17q12-20. ERBB2 encodes a member of the tyrosine kinase family. It is over expressed or amplified in several tumors, including breast, ovarian, and digestive tract tumors, and closely correlates with tumor occurrence, development, and prognosis [51]. Conversely, the over expression and amplification of ERBB2 is reportedly uncommon in RCC [52, 53]. However, Duzcan et al. [54] found that the levels of Top IIα and ERBB2 were correlated, and that they were co-amplified. Herein, Top IIα was found to be over expressed in type 2 PRCC, and located on the common aberration chromosome 3p24; ERBB2 is located at 17q12-20, which showed amplification, and exon chip detection moreover revealed ERBB2 mutations. This suggests that Top IIα and ERBB2 may jointly participate in the occurrence and development of PRCC, and that exon chip analyses may facilitate the discovery of mutated genes in PRCC.

Table 5. The 19 differentially missense mutated genes in type 1PRCC C vs. type 2 PRCC ($P < 0.05$)**

SNP_name	Chr	Alleles	Mutation (s)	Gene
exm330459	3p12.3	[C/G]	Missense_H75D	CNTN3
exm318874	3p21.2	[A/G]	Missense_R425C, Missense_R426C	VPRBP
exm506256	5q35.2	[A/G]	Missense_A328T, Missense_A328T, Missense_A328T	FGFR4
exm611166	7p15.2	[C/G]	Missense_R132S	HOXA11
exm693941	8p12	[A/G]	Missense_T2181I	TEX15
exm727114	8q24.3	[A/C]	Missense_L361R, Missense_L361R	EEF1D
exm919007	11q12.3	[G/C]	Missense_A866P	INTS5
exm940191	11q13.4	[A/G]	Missense_R142Q	DNAJB13
exm976848	12p13.3	[T/C]	Missense_R606Q	VWF
exm1185487	15q24-q25	[A/G]	Missense_D1086N, Missense_D1086N	AKAP13
exm1368709	17q25	[A/C]	Missense_H288Q	RFNG
exm1277466	17p13.3	[T/C]	Missense_P285S	OR1A1
exm1351674	17q25.1	[T/C]	Missense_T407M	GPR142
exm1352075	17q25.1	[T/G]	Missense_T282K	RAB37
exm1379777	18q11.2	[A/G]	Missense_A152T	TAF4B
exm1395964	19p13.3	[T/C]	Missense_A314V, Missense_A227V	MADCAM1
exm1529410	20p11.21	[T/C]	Missense_P297S	GZF1
exm1663015	Xq28	[T/C]	Missense_V377A	PNMA3

**Type 1 PRCC C vs. type 2 PRCC; Fisher's exact test. Abbreviations: PRCC, Papillary renal cell carcinoma; Chr., chromosome; SNP, single nucleotide polymorphism.

Using exome sequencing, we here found that the EEF1D, RFNG, GPR142, and RAB37 genes were located in different chromosomal regions in type 1 and 2 PRCC. RAB37, which is located at chromosome 17q25.1, more often showed gains in type 1 PRCC. Dobashi et al. [55] found that RAB37 was upregulated in RCC cells, and knockdown of RAB37 expression by specific siRNA caused significant reductions in cancer cell growth. Furthermore, Wu [56] also found that promoter/exon 1 methylation lead to down-regulation of hRAB37 in metastatic lung cancer, and that it may serve as a predictive biomarker of lung cancer progression. EEF1D, which is located at chromosome 8q24.3 and was more commonly mutated in type 2 PRCC, is also overexpressed in medulloblastoma [57] and right-sided colon cancer [58], and correlates with the invasive status of adriamycin-resistant variants of DLKP, a squamous lung cancer cell line [59]. Accordingly, we speculate that the mutations of RAB37 and EEF1D may play different roles in the development of type 1 and 2 PRCC.

In conclusion, our study shows that multiple gene mutations are present in PRCC. These gene mutations may provide clues regarding PRCC tumorigenesis and serve as a basis for future developments of targeted therapies against type 1 and 2 PRCC.

Acknowledgements

Supported by grants from the National Natural Science Foundation of China (NSFC, No. 81060383). We would like to thank Editage http://www.editage.cn/ for English language editing.

Disclosure of conflict of interest

None.

Address correspondence to: Drs. Hong Zou and Feng Li, Department of Pathology, Shihezi University School of Medicine, Key Laboratory of Xinjiang Endemic and Ethnic Diseases, Ministry of Education of China. E-mail: zouhong.patho@gmail.com (HZ); lifeng7855@126.com (FL)

References

[1] John N, Eble GS, Jonathan I, Epstein Isabell A, Sesterhenn. World health organization classification of tumors: pathology and genetics of tumors of the urinary system and male genital organs. Lyon: IARC Press; 2004.

[2] Delahunt B, Eble JN, McCredie MR, Bethwaite PB, Stewart JH and Bilous AM. Morphologic typing of papillary renal cell carcinoma: comparison of growth kinetics and patient survival in 66 cases. Hum Pathol 2001; 32: 590-595.
[3] Steffens S, Janssen M, Roos FC, Becker F, Schumacher S, Seidel C, Wegener G, Thuroff JW, Hofmann R, Stockle M, Siemer S, Schrader M, Hartmann A, Kuczyk MA, Junker K and Schrader AJ. Incidence and long-term prognosis of papillary compared to clear cell renal cell carcinoma--a multicentre study. Eur J Cancer 2012; 48: 2347-2352.
[4] Cheville JC, Lohse CM, Zincke H, Weaver AL and Blute ML. Comparisons of outcome and prognostic features among histologic subtypes of renal cell carcinoma. Am J Surg Pathol 2003; 27: 612-624.
[5] Ficarra V, Martignoni G, Galfano A, Novara G, Gobbo S, Brunelli M, Pea M, Zattoni F and Artibani W. Prognostic role of the histologic subtypes of renal cell carcinoma after slide revision. Eur Urol 2006; 50: 786-793; discussion 793-784.
[6] Gordon MS, Hussey M, Nagle RB, Lara PN Jr, Mack PC, Dutcher J, Samlowski W, Clark JI, Quinn DI, Pan CX and Crawford D. Phase II study of erlotinib in patients with locally advanced or metastatic papillary histology renal cell cancer: SWOG S0317. J Clin Oncol 2009; 27: 5788-5793.
[7] Patard JJ, Leray E, Rioux-Leclercq N, Cindolo L, Ficarra V, Zisman A, De La Taille A, Tostain J, Artibani W, Abbou CC, Lobel B, Guille F, Chopin DK, Mulders PF, Wood CG, Swanson DA, Figlin RA, Belldegrun AS and Pantuck AJ. Prognostic value of histologic subtypes in renal cell carcinoma: a multicenter experience. J Clin Oncol 2005; 23: 2763-2771.
[8] Ridge CA, Pua BB and Madoff DC. Epidemiology and staging of renal cell carcinoma. Semin Intervent Radiol 2014; 31: 3-8.
[9] Schmidt L, Duh FM, Chen F, Kishida T, Glenn G, Choyke P, Scherer SW, Zhuang Z, Lubensky I, Dean M, Allikmets R, Chidambaram A, Bergerheim UR, Feltis JT, Casadevall C, Zamarron A, Bernues M, Richard S, Lips CJ, Walther MM, Tsui LC, Geil L, Orcutt ML, Stackhouse T, Lipan J, Slife L, Brauch H, Decker J, Niehans G, Hughson MD, Moch H, Storkel S, Lerman MI, Linehan WM and Zbar B. Germline and somatic mutations in the tyrosine kinase domain of the MET proto-oncogene in papillary renal carcinomas. Nat Genet 1997; 16: 68-73.
[10] Farber LJ, Furge K and Teh BT. Renal cell carcinoma deep sequencing: recent developments. Curr Oncol Rep 2012; 14: 240-248.
[11] Kosaka T, Mikami S, Miyajima A, Kikuchi E, Nakagawa K, Ohigashi T, Nakashima J and Oya M. Papillary renal cell carcinoma: clinicopathological characteristics in 40 patients. Clin Exp Nephrol 2008; 12: 195-199.
[12] Antonelli A, Tardanico R, Balzarini P, Arrighi N, Perucchini L, Zanotelli T, Cozzoli A, Zani D, Cunico SC and Simeone C. Cytogenetic features, clinical significance and prognostic impact of type 1 and type 2 papillary renal cell carcinoma. Cancer Genet Cytogenet 2010; 199: 128-133.
[13] Yamanaka K, Miyake H, Hara I, Inoue TA, Hanioka K and Fujisawa M. Papillary renal cell carcinoma: a clinicopathological study of 35 cases. Int J Urol 2006; 13: 1049-1052.
[14] Margulis V, Tamboli P, Matin SF, Swanson DA and Wood CG. Analysis of clinicopathologic predictors of oncologic outcome provides insight into the natural history of surgically managed papillary renal cell carcinoma. Cancer 2008; 112: 1480-1488.
[15] Zucchi A, Novara G, Costantini E, Antonelli A, Carini M, Carmignani G, Cosciani Cunico S, Fontana D, Longo N, Martignoni G, Minervini A, Mirone V, Porena M, Roscigno M, Schiavina R, Simeone C, Simonato A, Siracusano S, Terrone C and Ficarra V. Prognostic factors in a large multi-institutional series of papillary renal cell carcinoma. BJU Int 2012; 109: 1140-1146.
[16] Mejean A, Hopirtean V, Bazin JP, Larousserie F, Benoit H, Chretien Y, Thiounn N and Dufour B. Prognostic factors for the survival of patients with papillary renal cell carcinoma: meaning of histological typing and multifocality. J Urol 2003; 170: 764-767.
[17] Allory Y, Ouazana D, Boucher E, Thiounn N and Vieillefond A. Papillary renal cell carcinoma. Prognostic value of morphological subtypes in a clinicopathologic study of 43 cases. Virchows Arch 2003; 442: 336-342.
[18] Waldert M, Haitel A, Marberger M, Katzenbeisser D, Ozsoy M, Stadler E and Remzi M. Comparison of type I and II papillary renal cell carcinoma (RCC) and clear cell RCC. BJU Int 2008; 102: 1381-1384.
[19] Wang L, Williamson SR, Wang M, Davidson DD, Zhang S, Baldridge LA, Du X and Cheng L. Molecular subtyping of metastatic renal cell carcinoma: implications for targeted therapy. Mol Cancer 2014; 13: 39.
[20] Al-Ahmadie HA, Alden D, Fine SW, Gopalan A, Touijer KA, Russo P, Reuter VE and Tickoo SK. Role of immunohistochemistry in the evaluation of needle core biopsies in adult renal cortical tumors: an ex vivo study. Am J Surg Pathol 2011; 35: 949-961.
[21] Williamson SR, Halat S, Eble JN, Grignon DJ, Lopez-Beltran A, Montironi R, Tan PH, Wang M, Zhang S, Maclennan GT, Baldridge LA and Cheng L. Multilocular cystic renal cell carcinoma: similarities and differences in immunopro-

file compared with clear cell renal cell carcinoma. Am J Surg Pathol 2012; 36: 1425-1433.
[22] Panousis D, Patsouris E, Lagoudianakis E, Pappas A, Kyriakidou V, Voulgaris Z, Xepapadakis G, Manouras A, Athanassiadou AM and Athanassiadou P. The value of TOP2A, EZH2 and paxillin expression as markers of aggressive breast cancer: relationship with other prognostic factors. Eur J Gynaecol Oncol 2011; 32: 156-159.
[23] Gao XH, Yu ZQ, Zhang C, Bai CG, Zheng JM and Fu CG. DNA topoisomerase II alpha: a favorable prognostic factor in colorectal caner. Int J Colorectal Dis 2012; 27: 429-435.
[24] Dekel Y, Frede T, Kugel V, Neumann G, Rassweiler J and Koren R. Human DNA topoisomerase II-alpha expression in laparoscopically treated renal cell carcinoma. Oncol Rep 2005; 14: 271-274.
[25] Ding S, Xing N, Lu J, Zhang H, Nishizawa K, Liu S, Yuan X, Qin Y, Liu Y, Ogawa O and Nishiyama H. Overexpression of Eg5 predicts unfavorable prognosis in non-muscle invasive bladder urothelial carcinoma. Int J Urol 2011; 18: 432-438.
[26] Liou GY, Zhang H, Miller EM, Seibold SA, Chen W and Gallo KA. Induced, selective proteolysis of MLK3 negatively regulates MLK3/JNK signalling. Biochem J 2010; 427: 435-443.
[27] Whitworth H, Bhadel S, Ivey M, Conaway M, Spencer A, Hernan R, Holemon H and Gioeli D. Identification of kinases regulating prostate cancer cell growth using an RNAi phenotypic screen. PLoS One 2012; 7: e38950.
[28] Chen J, Miller EM and Gallo KA. MLK3 is critical for breast cancer cell migration and promotes a malignant phenotype in mammary epithelial cells. Oncogene 2010; 29: 4399-4411.
[29] Mishra P, Senthivinayagam S, Rangasamy V, Sondarva G and Rana B. Mixed lineage kinase-3/JNK1 axis promotes migration of human gastric cancer cells following gastrin stimulation. Mol Endocrinol 2010; 24: 598-607.
[30] Martens-de Kemp SR, Nagel R, Stigter-van Walsum M, van der Meulen IH, van Beusechem VW, Braakhuis BJ and Brakenhoff RH. Functional genetic screens identify genes essential for tumor cell survival in head and neck and lung cancer. Clin Cancer Res 2013; 19: 1994-2003.
[31] Tang Y, Orth JD, Xie T and Mitchison TJ. Rapid induction of apoptosis during Kinesin-5 inhibitor-induced mitotic arrest in HL60 cells. Cancer Lett 2011; 310: 15-24.
[32] Marra E, Palombo F, Ciliberto G and Aurisicchio L. Kinesin spindle protein SiRNA slows tumor progression. J Cell Physiol 2013; 228: 58-64.
[33] Sun D, Lu J, Ding K, Bi D, Niu Z, Cao Q, Zhang J and Ding S. The expression of Eg5 predicts a poor outcome for patients with renal cell carcinoma. Med Oncol 2013; 30: 476.
[34] Kovalev AA, Tsvetaeva DA and Grudinskaja TV. Role of ABC-cassette transporters (MDR1, MRP1, BCRP) in the development of primary and acquired multiple drug resistance in patients with early and metastatic breast cancer. Exp Oncol 2013; 35: 287-290.
[35] Wang F, Wang XK, Shi CJ, Zhang H, Hu YP, Chen YF and Fu LW. Nilotinib enhances the efficacy of conventional chemotherapeutic drugs in CD34 (+) CD38 (-) stem cells and ABC transporter overexpressing leukemia cells. Molecules 2014; 19: 3356-3375.
[36] Zhao X, Guo Y, Yue W, Zhang L, Gu M and Wang Y. ABCC4 is required for cell proliferation and tumorigenesis in non-small cell lung cancer. Onco Targets Ther 2014; 7: 343-351.
[37] Walsh N, Larkin A, Kennedy S, Connolly L, Ballot J, Ooi W, Gullo G, Crown J, Clynes M and O'Driscoll L. Expression of multidrug resistance markers ABCB1 (MDR-1/P-gp) and ABCC1 (MRP-1) in renal cell carcinoma. BMC Urol 2009; 9: 6.
[38] Hour TC, Kuo YZ, Liu GY, Kang WY, Huang CY, Tsai YC, Wu WJ, Huang SP and Pu YS. Downregulation of ABCD1 in human renal cell carcinoma. Int J Biol Markers 2009; 24: 171-178.
[39] Delektorskaya VV, Golovkov DA and Kushlinskii NE. Clinical significance of levels of molecular biological markers in zones of invasive frontline of colorectal cancer. Bull Exp Biol Med 2008; 146: 616-619.
[40] Ohlund D, Lundin C, Ardnor B, Oman M, Naredi P and Sund M. Type IV collagen is a tumour stroma-derived biomarker for pancreas cancer. Br J Cancer 2009; 101: 91-97.
[41] Ryschich E, Khamidjanov A, Kerkadze V, Buchler MW, Zoller M and Schmidt J. Promotion of tumor cell migration by extracellular matrix proteins in human pancreatic cancer. Pancreas 2009; 38: 804-810.
[42] Kato Y, Sakai N, Baba M, Kaneko S, Kondo K, Kubota Y, Yao M, Shuin T, Saito S, Koshika S, Kawase T, Miyagi Y, Aoki I and Nagashima Y. Stimulation of motility of human renal cell carcinoma by SPARC/Osteonectin/BM-40 associated with type IV collagen. Invasion Metastasis 1998; 18: 105-114.
[43] Nakayama Y, Naito S, Ryuto M, Hata Y, Ono M, Sueishi K, Komiyama S, Itoh H and Kuwano M. An in vitro invasion model for human renal cell carcinoma cell lines mimicking their metastatic abilities. Clin Exp Metastasis 1996; 14: 466-474.
[44] Lohi J, Korhonen M, Leivo I, Kangas L, Tani T, Kalluri R, Miner JH, Lehto VP and Virtanen I. Expression of type IV collagen alpha1(IV)-alpha6(IV) polypeptides in normal and devel-

oping human kidney and in renal cell carcinomas and oncocytomas. Int J Cancer 1997; 72: 43-49.
[45] Sanders ME, Mick R, Tomaszewski JE and Barr FG. Unique patterns of allelic imbalance distinguish type 1 from type 2 sporadic papillary renal cell carcinoma. Am J Pathol 2002; 161: 997-1005.
[46] Matsuda D, Khoo SK, Massie A, Iwamura M, Chen J, Petillo D, Wondergem B, Avallone M, Kloostra SJ, Tan MH, Koeman J, Zhang Z, Kahnoski RJ; French Kidney Cancer Study Group, Baba S, Teh BT. Identification of copy number alterations and its association with pathological features in clear cell and papillary RCC. Cancer Lett 2008; 272: 260-267.
[47] Klatte T, Pantuck AJ, Said JW, Seligson DB, Rao NP, LaRochelle JC, Shuch B, Zisman A, Kabbinavar FF and Belldegrun AS. Cytogenetic and molecular tumor profiling for type 1 and type 2 papillary renal cell carcinoma. Clin Cancer Res 2009; 15: 1162-1169.
[48] Yang XJ, Tan MH, Kim HL, Ditlev JA, Betten MW, Png CE, Kort EJ, Futami K, Furge KA, Takahashi M, Kanayama HO, Tan PH, Teh BS, Luan C, Wang K, Pins M, Tretiakova M, Anema J, Kahnoski R, Nicol T, Stadler W, Vogelzang NG, Amato R, Seligson D, Figlin R, Belldegrun A, Rogers CG and Teh BT. A molecular classification of papillary renal cell carcinoma. Cancer Res 2005; 65: 5628-5637.
[49] Lopez-Beltran A, Montironi R, Egevad L, Caballero-Vargas MT, Scarpelli M, Kirkali Z and Cheng L. Genetic profiles in renal tumors. Int J Urol 2010; 17: 6-19.
[50] Cheng L, Zhang S, MacLennan GT, Lopez-Beltran A and Montironi R. Molecular and cytogenetic insights into the pathogenesis, classification, differential diagnosis, and prognosis of renal epithelial neoplasms. Hum Pathol 2009; 40: 10-29.
[51] Menard S, Casalini P, Campiglio M, Pupa S, Agresti R and Tagliabue E. HER2 overexpression in various tumor types, focussing on its relationship to the development of invasive breast cancer. Ann Oncol 2001; 12 Suppl 1: S15-19.
[52] Wang H, Liu C, Han J, Zhen L, Zhang T, He X, Xu E and Li M. HER2 expression in renal cell carcinoma is rare and negatively correlated with that in normal renal tissue. Oncol Lett 2012; 4: 194-198.
[53] Latif Z, Watters AD, Bartlett JM, Underwood MA and Aitchison M. Gene amplification and overexpression of HER2 in renal cell carcinoma. BJU Int 2002; 89: 5-9.
[54] Duzcan F, Duzcan SE, Sen S, Yorukoglu K, Caner V, Sen Turk N, Cetin GO, Kelten C, Tuna B, Sarsik B and Tepeli E. Expression and amplification of Topoisomerase-2alpha in type 1 and type 2 papillary renal cell carcinomas and its correlation with HER2/neu amplification. Pathol Oncol Res 2011; 17: 697-703.
[55] Dobashi S, Katagiri T, Hirota E, Ashida S, Daigo Y, Shuin T, Fujioka T, Miki T and Nakamura Y. Involvement of TMEM22 overexpression in the growth of renal cell carcinoma cells. Oncol Rep 2009; 21: 305-312.
[56] Wu CY, Tseng RC, Hsu HS, Wang YC and Hsu MT. Frequent down-regulation of hRAB37 in metastatic tumor by genetic and epigenetic mechanisms in lung cancer. Lung Cancer 2009; 63: 360-367.
[57] De Bortoli M, Castellino RC, Lu XY, Deyo J, Sturla LM, Adesina AM, Perlaky L, Pomeroy SL, Lau CC, Man TK, Rao PH and Kim JY. Medulloblastoma outcome is adversely associated with overexpression of EEF1D, RPL30, and RPS20 on the long arm of chromosome 8. BMC Cancer 2006; 6: 223.
[58] Shen H, Huang J, Pei H, Zeng S, Tao Y, Shen L, Zeng L and Zhu H. Comparative proteomic study for profiling differentially expressed proteins between Chinese left- and right-sided colon cancers. Cancer Sci 2013; 104: 135-141.
[59] Keenan J, Murphy L, Henry M, Meleady P and Clynes M. Proteomic analysis of multidrug-resistance mechanisms in adriamycin-resistant variants of DLKP, a squamous lung cancer cell line. Proteomics 2009; 9: 1556-1566.